World Journal of Gastroenterology

Online Submissions: http://www.wjgnet.com/1007-9327office
wjg@wjgnet.com
doi:10.3748/wjg.v18.i28.3673

World J Gastroenterol 2012 July 28; 18(28): 3673-3680
ISSN 1007-9327 (print) ISSN 2219-2840 (online)

ORIGINAL ARTICLE

Intraductal neoplasm of the intrahepatic bile duct: Clinicopathological study of 24 cases

Yoshiki Naito, Hironori Kusano, Osamu Nakashima, Eiji Sadashima, Satoshi Hattori, Tomoki Taira, Akihiko Kawahara, Yoshinobu Okabe, Kazuhide Shimamatsu, Jun Taguchi, Seiya Momosaki, Koji Irie, Rin Yamaguchi, Hiroshi Yokomizo, Michiko Nagamine, Seiji Fukuda, Shinichi Sugiyama, Naoyo Nishida, Koichi Higaki, Munehiro Yoshitomi, Masafumi Yasunaga, Koji Okuda, Hisafumi Kinoshita, Masamichi Nakayama, Makiko Yasumoto, Jun Akiba, Masayoshi Kage, Hirohisa Yano

Yoshiki Naito, Hironori Kusano, Osamu Nakashima, Masamichi Nakayama, Makiko Yasumoto, Jun Akiba, Hirohisa Yano, Departments of Pathology, Kurume University School of Medicine, Kurume 830-0011, Japan
Eiji Sadashima, Satoshi Hattori, Biostatistics Center, Kurume University, Kurume 830-0011, Japan
Tomoki Taira, Akihiko Kawahara, Masayoshi Kage, Department of Diagnostic Pathology, Kurume University Hospital, Kurume 830-0011, Japan
Yoshinobu Okabe, Division of Gastroenterology, Department of Medicine, Kurume University School of Medicine, Kurume 830-0011, Japan
Kazuhide Shimamatsu, Department of Pathology, Omuta City General Hospital, Omuta 836-8567, Japan
Jun Taguchi, Department of Pathology, Asakura Medical Association Hospital, Fukuoka 838-0069, Japan
Seiya Momosaki, Department of Pathology, National Hospital Organization Kyushu Medical Center, Fukuoka 810-8563, Japan
Koji Irie, Department of Pathology, Shin-Koga Hospital, Tenjinkai, 120 Tenjincho, Kurume 830-0033, Japan
Rin Yamaguchi, Department of Pathology, Kurume University Medical Center, 155-1 Kokubumachi, Kurume 839-0863, Japan
Hiroshi Yokomizo, Department of Surgery, Japanese Red Cross Kumamoto Hospital, Kumamoto 861-8520, Japan
Michiko Nagamine, Seiji Fukuda, Department of Pathology, Japanese Red Cross Kumamoto Hospital, Kumamoto 861-8520, Japan
Shinichi Sugiyama, Division of Surgery, Saiseikai Kumamoto Hospital, Kumamoto 861-4193, Japan
Naoyo Nishida, Koichi Higaki, Department of Pathology, St Mary's Hospital, Kurume 830-8543, Japan
Munehiro Yoshitomi, Masafumi Yasunaga, Koji Okuda, Hisafumi Kinoshita, Department of Surgery, Kurume University School of Medicine, Kurume 830-0011, Japan
Author contributions: Naito Y, Nakashima O and Kusano H performed the majority of the experiments; Yano H was involved in editing the manuscript; all authors provided the collection of all the human material and advised for the manuscript.
Correspondence to: Yoshiki Naito, MD, PhD, Department of Pathology, Kurume University School of Medicine, 67 Asahimachi, Kurume 830-0011, Japan. nyoshiki@med.kurume-u.ac.jp
Telephone: +81-942-317546 Fax: +81-942-320905
Received: November 14, 2011 Revised: March 27, 2012
Accepted: March 29, 2012
Published online: July 28, 2012

Abstract

AIM: To investigate the clinicopathological features of intraductal neoplasm of the intrahepatic bile duct (INihB).

METHODS: Clinicopathological features of 24 cases of INihB, which were previously diagnosed as biliary papillomatosis or intraductal growth of intrahepatic biliary neoplasm, were reviewed. Mucin immunohistochemistry was performed for mucin (MUC)1, MUC2, MUC5AC and MUC6. Ki-67, P53 and β-catenin immunoreactivity were also examined. We categorized each tumor as adenoma (low grade), borderline (intermediate grade), and malignant (carcinoma *in situ*, high grade including tumors with microinvasion).

RESULTS: Among 24 cases of INihB, we identified 24 tumors. Twenty of 24 tumors (83%) were composed of a papillary structure; the same feature observed in intraductal papillary neoplasm of the bile duct (IPNB). In contrast, the remaining four tumors (17%) showed both tubular and papillary structures. In three of the four tumors (75%), macroscopic mucin secretion was limited but microscopic intracellular mucin was evident. Histologically, 16 tumors (67%) were malignant, three (12%) were borderline, and five (21%) were adenoma. Microinvasion was found in four cases (17%). Immunohistochemical analysis revealed that MUC1 was not expressed in the borderline/adenoma group but was

expressed only in malignant lesions (P = 0.0095). Ki-67 labeling index (LI) was significantly higher in the malignant group than in the borderline/adenoma group (22.2 ± 15.5 *vs* 7.5 ± 6.3, P < 0.01). In the 16 malignant cases, expression of MUC5AC showed borderline significant association with high Ki-67 LI (P = 0.0622). Nuclear expression of β-catenin was observed in two (8%) of the 24 tumors, and these two tumors also showed MUC1 expression. P53 was negative in all tumors.

CONCLUSION: Some cases of INihB have a tubular structure, and are subcategorized as IPNB with tubular structure. MUC1 expression in INihB correlates positively with degree of malignancy.

Key words: Intraductal biliary neoplasm; Intraductal papillary neoplasm of the bile duct; Intraductal tubular neoplasm of the bile duct; Intraductal tubulopapillary neoplasm of the bile duct; Mucin expression

Peer reviewer: Dr. George Sgourakis, 2nd Surgical Department, Surgical Oncology Unit, Red Cross Hospital, 11 Mantzarou Str, 15451 Athens, Greece

Naito Y, Kusano H, Nakashima O, Sadashima E, Hattori S, Taira T, Kawahara A, Okabe Y, Shimamatsu K, Taguchi J, Momosaki S, Irie K, Yamaguchi R, Yokomizo H, Nagamine M, Fukuda S, Sugiyama S, Nishida N, Higaki K, Yoshitomi M, Yasunaga M, Okuda K, Kinoshita H, Nakayama M, Yasumoto M, Akiba J, Kage M, Yano H. Intraductal neoplasm of the intrahepatic bile duct: Clinicopathological study of 24 cases. *World J Gastroenterol* 2012; 18(28): 3673-3680 Available from: URL: http://www.wjgnet.com/1007-9327/full/v18/i28/3673.htm DOI: http://dx.doi.org/10.3748/wjg.v18.i28.3673

INTRODUCTION

Mucin-producing tumors arising from the bile duct have been reported previously[1-5], but as a disease category, consensus has not yet been reached. Recently, Shibahara *et al*[6] and Zen *et al*[7] have contributed to the development of the concept of papillary tumors in the bile duct that resemble intraductal papillary mucinous neoplasm of the pancreas (IPMN-P) and pancreatic intraepithelial neoplasia. These bile duct tumors show papillary proliferation in the bile duct with mucin secretion, and are considered as intraductal papillary neoplasm of the bile duct (IPN-B), that is, the biliary counterpart of IPMN-P[8,9]. Recent studies have indicated that IPN-B could be subcategorized according to the results of mucin immunohistochemistry[6,7], and the similarity of IPNB and IPMN-P has also been described.

In our current study, we conducted histological and immunohistochemical re-examination of 24 cases of intraductal neoplasm of the intrahepatic bile duct (INihB), which were previously reported as biliary papillomatosis or intraductal growth type of intrahepatic biliary neoplasm[10-13].

MATERIALS AND METHODS

Definition of INihB

We defined INihB as a tumor that (1) was localized in the liver; (2) arose within the intrahepatic bile duct; (3) had a major lesion that was noninfiltrative and showed an intraductal proliferation pattern; and (4) clinicopathologically communicated with the surrounding bile duct.

Tissue samples

We identified 24 cases of INihB from the medical record at Kurume University Hospital and affiliated institutions. These cases were previously diagnosed as intraductal intrahepatic biliary neoplasm or biliary papillomatosis[13]. Tissue sections of 4 μm thickness were prepared from paraffin-embedded tissue samples, and stained with hematoxylin and eosin (HE) in the usual manner. The slides were reviewed by the three pathologists (YN, HK and ON).

Degree of malignancy of intrahepatic bile duct

HE-stained sections were reviewed and each tumor was categorized into three groups according to the degree of malignancy by using the criteria in IPMN-P[8]: adenoma (low grade), borderline (intermediate grade), and malignant (carcinoma *in situ* and high grade). Tumors with microinvasion were categorized as malignant.

Immunohistochemistry

Paraffin-embedded, 4-μm-thick sections on a coated glass slides were stained by using the BenchMark XT (Ventata Automated Systems, Inc., Tucson, AZ, United States) with the following antibodies: mucin (MUC)1 (mouse monoclonal, Ma695, dilution 1:100; Novocastra, Newcastle, United Kingdom); MUC2 (mouse monoclonal, Ccp58, dilution 1:100; Novocastra); MUC5AC (mouse monoclonal, CLH2, dilution 1:100; Novocastra); MUC6 (mouse monoclonal, CLH5, dilution 1:50; Novocastra); p53 (mouse monoclonal, DO-7, dilution 1:200; Novocastra); β-catenin (mouse monoclonal, β-catenin-1, dilution 1:200; Dako, Glostrup, Denmark); and Ki-67 (mouse monoclonal, MIB-1, dilution 1:100; Dako). This automated system uses the streptavidin-biotin complex method with DAB as a chromogen (Ventana iVIEW DAB Detection Kit).

Regarding the MUC profile, we evaluated cytoplasmic and luminal surface staining by referring to the method of Shibahara *et al*[6], and the cells were considered positive when either one or both of the two components were stained. The percentage of positively stained neoplastic cells was also calculated and graded as follows: -, < 5% of the neoplastic cells were stained; +, ≥ 5% and < 20% were stained; 2+, ≥ 20% and < 50% were stained, and 3+, ≥ 50% were stained. These evaluations were conducted by three pathologists (YN, HK and ON). Positivity of p53 and β-catenin were defined by distinct and diffuse nuclear staining among the neoplastic cells. Ki-67 staining was counted on a minimum of 1000 tumor cells and Ki-67 labeling index (LI) was calculated as the per-

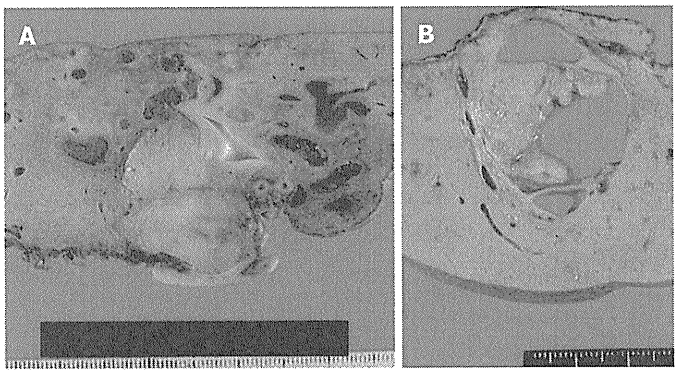

Figure 1 Gross findings. A: Duct-ectatic type. Tumor filled the dilated intrahepatic bile duct. Surrounding bile duct was also dilated; B: Cystic type. Cystic dilatation of intrahepatic bile duct. Papillary tumor was found in the dilated intrahepatic bile duct. Significant retention of mucin was observed.

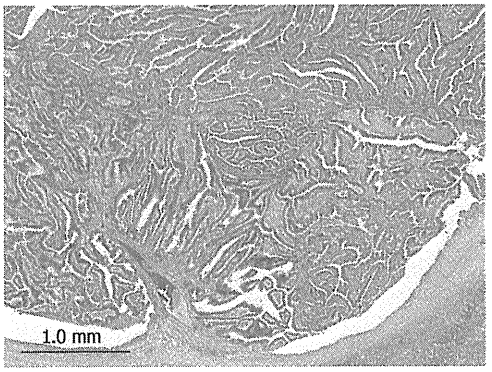

Figure 2 Histopathology of intraductal neoplasm of the intrahepatic bile duct. Tumor shows papillary proliferation within the dilated bile duct (hematoxylin and eosin stain, × 20).

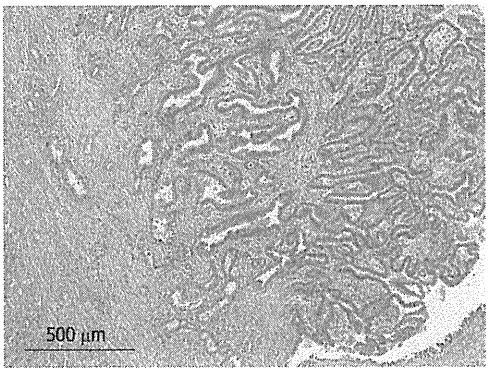

Figure 3 Microinvasion of tumor. Tumor cells infiltrating into the bile duct wall (hematoxylin and eosin stain, × 40).

centage of positively stained cells to total cells.

Statistical analysis

Associations of Ki-67 LI and expression of MUC family (0, 1+ or 2+, 3+) with the degree of malignancy (adenoma, borderline or malignant), and association between Ki-67 LI and MUC profile were examined using the Kruskal-Wallis test and Fisher's exact test. To apply Fisher's exact test, we classified MUC profile into two categories of 0 or 1+ and 2+ or 3+. Association was considered significant when $P < 0.05$. All the statistical analyses were conducted by SAS version 9.12 (SAS Institute Inc., Cary, NC, United States) and R version 2.9.0.

RESULTS

Patients with INihB

We identified 24 tumors in 24 patients. Clinical findings are summarized in Table 1. Median age at the initial diagnosis was 64 years (mean: 63.0 ± 8.1), and the male: female ratio was 1:1. Sixteen tumors (67%) were located in the left lobe. Nineteen tumors (79%) were cystic type associated with mucin hypersecretion, and five tumors (21%) were duct-ectatic type without mucin hypersecretion (Figure 1). Twenty tumors (83%) had papillary structures in the bile duct as IPNB (Figure 2). The remaining four tumors (17%) presented the following features: the tumor was localized and proliferated in the bile duct, and the tumor showed both tubular and papillary structures. In three of the four tumors (75%), macroscopic mucin secretion was limited but microscopic intracellular mucin was evident. Histologically, 16 tumors (67%) were malignant, three (12%) were borderline, and five (21%) were adenoma. Microinvasion was found in four tumors (21%) (Figure 3), and these were categorized as malignant. There was no ovarian-like stroma in any cases.

Four tumors (17%) were composed of both papillary and tubular structures (Table 2). Histological findings of four patients were similar to those of intraductal tubulopapillary neoplasm (ITPN-P)[14] or intraductal tubular neoplasm of the pancreas (ITN-P)[15]. One of these four cases was previously reported as a biliary papillomatosis by Taguchi *et al*[13], and the tumor spread from the intrahepatic to extrahepatic bile duct. Another two cases also showed extension of tumor with bile duct dilation. However, the remaining tumor was cystic type and macroscopic mucin hypersecretion was evident. Among tubular structures, a pyloric gland-like structure (Figure 4) was prominent. Three cases were not malignant, but one tumor showed cytological atypia, such as enlarged nuclei with pleomorphism, and was considered as malignant (Figure 5). Atypi-

Table 1 Clinicopathological features of 24 patients with intraductal neoplasm of the intrahepatic bile duct

Age (yr), median (mean ± SD)	64.0 (63.0 ± 8.1)
Gender, *n* (%)	
Male	12 (50)
Female	12 (50)
Location, *n* (%)	
Left lobe	16 (67)
Right lobe	8 (33)
Tumor size (cm), median (mean ± SD)	30 (42.2 ± 26.6)
Macroscopic findings of bile duct, *n* (%)	
Duct-ectatic	5 (21)
Cystic	19 (79)
Macroscopic mucin hypersecretion, *n* (%)	
Present	19 (79)
Absent	5 (21)
Histological structure pattern, *n* (%)	
Papillary	20 (83)
Tubular and papillary	4 (17)
Histological grade, *n* (%)	
Malignant	16 (67)
Borderline	3 (12)
Adenoma	5 (21)
Microinvasion, *n* (%)	
Present	4 (17)
Absent	20 (83)

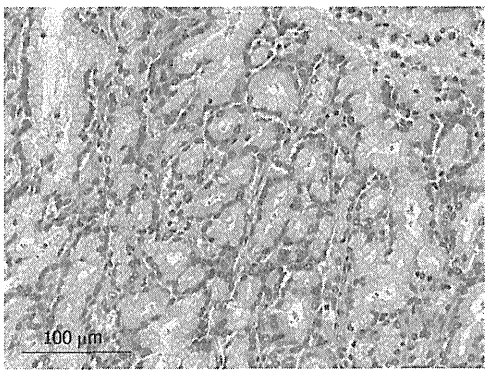

Figure 4 Tubular structure within intraductal neoplasm of the intrahepatic bile duct. Cells with intracellular mucin and mild atypia forming a pyloric gland-like structure (hematoxylin and eosin stain, × 200).

cal cells lining the tubular structure were cuboidal or columnar with little or no cytoplasmic mucin. None of these four cases were associated with tumor invasion.

Immunohistochemical analysis of INihB

Immunohistochemical findings are shown in Table 3. MUC1 was not expressed in the borderline/adenoma group but was expressed in malignant lesions ($P = 0.0095$). No specific pattern of expression was observed for other MUC family members. The Ki-67 LI was significantly higher in the malignant group than in the borderline/adenoma group (22.2 ± 15.5 *vs* 7.5 ± 6.3, $P < 0.01$, Figure 6A). In the 16 malignant tumors, there was an association of borderline significance between expression of MUC5AC and higher Ki-67 LI ($P = 0.0622$, Figure 6B). Expression of β-catenin was found in two of the 24 tumors (8%, Figure 7), and these two tumors were also positive for MUC1. P53 was negative in all 24 tumors.

Table 2 Clinicopathological findings of intraductal neoplasm of the intrahepatic bile duct with papillary and tubular structure in four patients

	Case 1	Case 2	Case 3[1]	Case 4
Age (yr)	77	49	63	52
Gender	Male	Female	Male	Male
Location	Left lobe			
Tumor size (cm)	10	2	6	2.6
Mucin produced macroscopically	Absent			Present
Macroscopic findings	Duct-ectatic type			Cystic
Histopathological grade	Malignant	Borderline	Adenoma	Adenoma
Microinvasion	Absent			
Mucin immunohistochemistry				
MUC1	3+	-	-	1+
MUC2	-	-	-	-
MUC5AC	-	1+	-	-
MUC6	3+	3+	+	3+

[1]Has been reported as biliary papillomatosis.

Table 3 Immunohistochemical features of 24 cases of intraductal neoplasm of the intrahepatic bile duct

	Malignant *n* (16.67%)	Borderline *n* (3.12%)/ adenoma *n* (5.21%)
MUC1[1]		
3+ (38%)	9 (56)	0
2+ (0%)	0	0
1+/- (62%)	7 (44)	8 (100)
MUC2		
3+ (13%)	1 (6)	2 (25)
2+ (4%)	1 (6)	0
1+/- (83%)	14 (88)	6 (75)
MUC5AC		
3+ (46%)	7 (44)	4 (50)
2+ (12%)	2 (12)	1 (13)
1+/- (42%)	7 (44)	3 (37)
MUC6		
3+ (46%)	4 (25)	5 (63)
2+ (12%)	4 (25)	1 (22)
1+/- (44%)	8 (50)	2 (25)
Proliferation		
Ki-67 (LI, %, mean ± SD)[2]	22.2 ± 15.5	7.5 ± 6.3
Genetic status		
TP53 overexpression	0	0
β-catenin nuclear expression (17%)[3]	2 (13)	0

[1]MUC1 expression was exhibited only in the malignant group ($P = 0.0095$); [2]Ki-67 was significantly higher in malignant cases than in borderline/adenoma patients ($P < 0.01$); [3]β-catenin expression was observed only in the cases with MUC1 expression. LI: Labeling index.

DISCUSSION

Many studies have been conducted on IPMN-P, and histomorphological criteria for diagnosis have been determined[8]. Regarding similar lesions in the bile duct, the definition of IPNB[7] and mucin-producing bile duct tumors[6] is proposed as a new conceptual framework

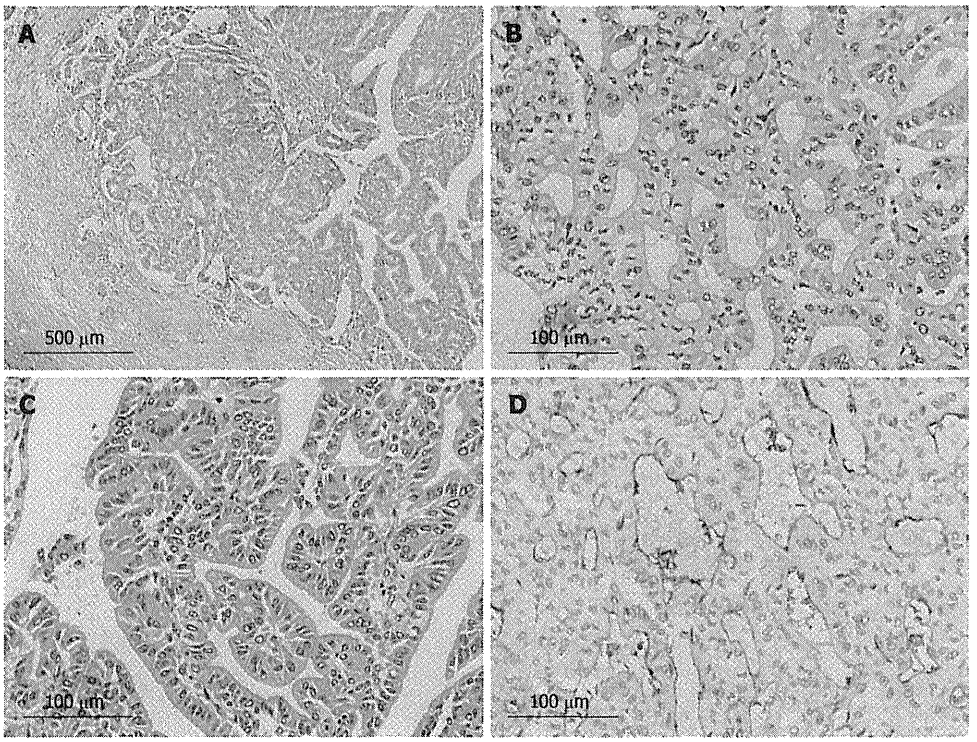

Figure 5 Histology of intraductal neoplasm of the intrahepatic bile duct with papillary and tubular structure (case 1). A: Histological structure was mainly tubular, but papillary structure was also present [hematoxylin and eosin (HE) stain, × 40]; B: Tubular structure (HE stain, × 200); C: Papillary structure (HE stain, × 200); D: Tumor cells were positive for mucin (MUC)1 immunohistochemistry (MUC1 stain, × 200).

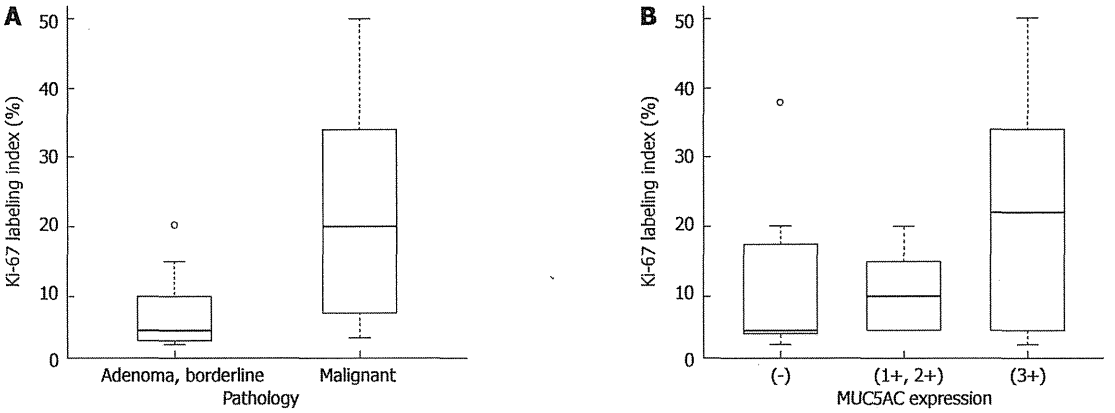

Figure 6 Box plot for Ki-67 labeling index by histological degree of malignancy and MUC5AC expression. A: The Ki-67 labeling index (LI) was significantly higher in the malignant group than in the benign/borderline group; B: There was an association with borderline significance between MUC5AC expression and Ki-67 LI (P = 0.0622). MUC: Mucin.

of biliary intraductal neoplasms. These biliary lesions present the same histological features of IPMN-P, and Zen *et al*[16,17] divided them into four categories, namely, pancreaticobiliary type, intestinal type, gastric type, and oncocytic type. In contrast, Shibahara *et al*[6] subclassified the lesions into two distinct categories, namely, columnar type and cuboidal type. Columnar type resembles intestinal type, and cuboidal type resembles pancreaticobiliary type or intraductal oncocytic papillary neoplasm, and they hypothesized that these two categories could be the biliary counterparts of IPMN-P.

Among our 24 cases of INihB, 19 cases (79%) were the cystic type that was proposed by Shibahara *et al*[6], and this type is known as a biliary cystic tumor. Devaney *et al*[18] reported that ovarian-like stroma was observed in 85% of the adenoma and 28% of the adenocarcinoma tumors. However, none of our cases had ovarian-like stroma. The presence or absence of ovarian-like stroma is an important factor for the classification of IPNB. Recently, Zen *et al*[17] proposed that biliary cystic tumor could be a cystic variant of IPNB, having bile duct communication and absence of ovarian-like stroma. Based on our

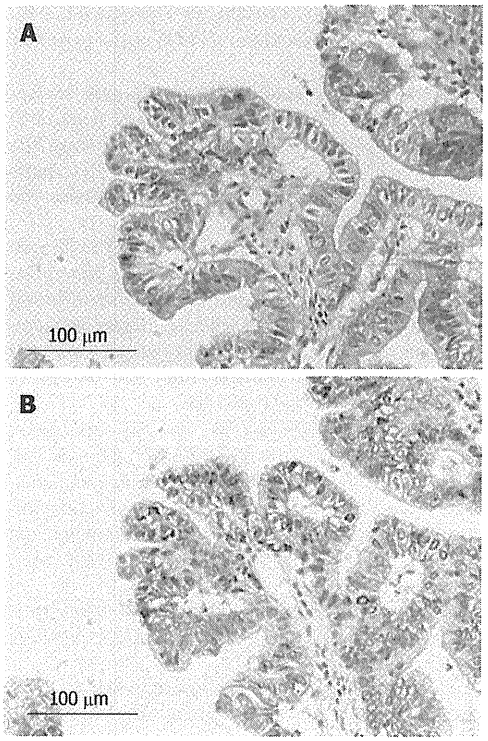

Figure 7 Nuclear expression of β-catenin in pancreaticobiliary type. A: Hematoxylin and eosin stain, × 200; B: β-catenin stain, × 200.

findings, the cystic type reported by Shibahara *et al*[6] and biliary cystic variant of IPNB reported by Zen *et al*[16] are the most common type among INihB, and they can be recognized by their characteristic macroscopic findings, that is, a cystic change with mucin hypersecretion, even though the tumors have ovarian-like stroma.

In our current study, 20 of 24 INihB tumors (83%) showed purely papillary proliferation that is a morphological feature of IPMN-P, and we diagnosed them as IPNB. In contrast, both papillary and tubular structures were present in the remaining four tumors (17%), and three of these four tumors were duct-ectatic type without macroscopic mucin secretion. These features are common findings in ITN-P or ITPN-P, which are rare diseases[15,19-24]. These tubulopapillary tumors can be distinctly subcategorized in INihB based on their characteristic macroscopic and histological findings. Intraductal neoplasms with a tubular structure have been reported in the pancreatic area. Albores-Saavedra *et al*[19] reported that tumors with a tubular structure included: (1) glands resembling pyloric glands; (2) glands lined by cells with no cytoplasmic mucin and with mild nuclear atypia; and (3) glands lined by pink oncocytic cells. Recently, Yamaguchi *et al*[14] proposed the concept of ITPN-P and defined nine diagnostic criteria. Similarly, some authors have described intraductal lesions in which IPNB with formation of the tubular structure is regarded as intraductal tubular neoplasm of the bile duct (ITNB)[25,26]. In our four cases, we observed morphological similarity with ITN-P or ITPN-P. In particular, Case 1 consisted mainly of a tubular structure and some papillary patterns, and the neoplastic cells were markedly atypical. In addition, immunohistochemical results were MUC1(+) and MUC5AC(-), which were different from ITN-P. Our case 1 was considered as an ITPN-B subcategory. As discussed above, IPNB contained IPNB with a tubular structure, although small in number, and there might be cases with similar characteristics to ITN-P or ITPN-P.

We also examined Ki-67 and p53 immunoreactivity in the 24 cases of INihB. Ki-67 expression differed significantly between malignant and borderline/adenoma (22.2 ± 15.5 *vs* 7.5 ± 6.3, $P < 0.01$), but P53 was negative in all cases. Based on these data, Ki-67 LI correlates with the degree of malignancy in INihB. Shibahara *et al*[6] reported significantly high Ki-67 expression and poorer prognosis in the columnar type than in the cuboidal type. In this study, we also investigated the relationship between MUC1/MUC5AC immunostaining and malignant potential. Some studies have reported that the pancreatobiliary type IPMN-P, which is positive for MUC1, is highly malignant[8]. Other studies have suggested that MUC1 contributes significantly to tumor growth and metastasis, and that downregulation of MUC1 protein expression decreases the metastatic potential of pancreatic adenocarcinoma[27]. The association between MUC1 and malignant potential has also been suggested in cholangiocarcinoma[28]. Although we did not find a significant association between MUC5AC expression and the degree of malignancy or cell proliferation potential, there was a borderline association between the higher expression of MUC5AC and the higher Ki-67 LI in the malignant group. Some authors also have reported that MUC5AC is more strongly expressed in advanced tumors[17,28]. Thus, we suggest that expression of MUC1 and MUC5AC is related, MUC1 more strongly so than MUC5AC, to the degree of malignancy in INihB.

Nuclear expression of β-catenin was found in 8% of INihB (2/24), and MUC1 was also positive in these cases. β-catenin is a mediator in the canonical Wnt signal transduction pathway[29] and activation of the Wnt pathway is associated with high proliferation and dedifferentiation in human biliary tumors[30]. Nuclear accumulation of β-catenin was reported in 15% of intrahepatic cholangiocarcinomas (Sugimachi *et al*[31]); 25% of IPN-B, 20% of IPN-B associated with intrahepatic cholangiocarcinoma, and 0% of biliary intraepithelial neoplasms (Itatsu *et al*[32]); and 25% of IPN-B (Abraham *et al*[33]). The Wnt signaling pathway is frequently activated in biliary neoplasms[32]. We believe when dealing with INihB one should consider performing immunohistochemical staining for MUC1 and β-catenin, in addition to histomorphological examination, to evaluate malignant potential of the tumor.

In conclusion, we propose the concept of INihB that includes IPNB and IPNB with tubular structure subcategories, that is, ITNB and intraductal tubulopapillary neoplasm of the bile duct. IPNB with tubular structure is rare, and (1) is mostly duct-ectatic without macroscopic mucin hypersecretion; and (2) histologically, has both

papillary and tubular structures. In INihB, MUC1 expression correlates positively with the degree of malignancy and cell proliferation potential. MUC5AC expression also correlates with the degree of malignancy, although the relationship is less robust. Further pathological and molecular studies are necessary to clarify the characteristics of INihB.

COMMENTS

Background

The clinicopathological characteristics of intraductal neoplasm of the intrahepatic bile duct (INihB) remains unclear. In this article, the authors present the clinicopathological features of 24 cases of INihB.

Research frontiers

Some studies have reported that the pancreatobiliary-type intraductal papillary mucinous neoplasm (IPMN-P), which is positive for mucin (MUC)1 expression, is highly malignant, and other studies have suggested that MUC1 contributes significantly to tumor growth and metastasis, and that downregulation of MUC1 protein expression decreases the metastatic potential of pancreatic adenocarcinoma. The association between MUC1 and malignant potential has also been suggested in cholangiocarcinoma. Some authors have reported that MUC5AC is more strongly expressed by advanced tumors. In this study, the authors demonstrated that MUC1 and MUC5AC expression may be related to the malignant potential of INihB.

Innovations and breakthroughs

Recent reports have highlighted the relationship between MUC profile and malignancy potential. In particular, the authors investigated the relationship between MUC1/MUC5AC immunohistochemical staining and Ki-67 labeling index.

Applications

This study offers a better understanding of clinicopathological characteristics of INihB and a potential strategy to predict tumor behavior for better patient care.

Terminology

MUC1/MUC5AC are mucin proteins in the pancreatobiliary/gastric epithelium, respectively. It has been suggested that these proteins play an important role in tumor growth and metastasis in pancreatobiliary disease.

Peer review

Immunohistochemical analysis revealed that Ki-67 expression in the 24 INihBs was significantly high in the malignant group. MUC staining showed that MUC1 was not expressed in the borderline/adenoma group but was expressed only in malignant lesions, and the Ki-67 labeling index was significantly higher in the malignant group than in the borderline/adenoma group. These results may represent a mechanism of MUC protein in tumor growth, that is, malignant potential of the tumor.

REFERENCES

1 **Ohtsubo K**, Ohta H, Sakai J, Mouri H, Nakamura S, Ikeda T, Kifune K, Yoshikawa J, Harada K, Nakanuma Y, Watanabe H, Motoo Y, Okai T, Sawabu N. Mucin-producing biliary papillomatosis associated with gastrobiliary fistula. *J Gastroenterol* 1999; **34**: 141-144

2 **Lim JH**, Kim YI, Park CK. Intraductal mucosal-spreading mucin-producing peripheral cholangiocarcinoma of the liver. *Abdom Imaging* 2000; **25**: 89-92

3 **Sakamoto E**, Hayakawa N, Kamiya J, Kondo S, Nagino M, Kanai M, Miyachi M, Uesaka K, Nimura Y. Treatment strategy for mucin-producing intrahepatic cholangiocarcinoma: value of percutaneous transhepatic biliary drainage and cholangioscopy. *World J Surg* 1999; **23**: 1038-1043; discussion 1043-1044

4 **Kokubo T**, Itai Y, Ohtomo K, Itoh K, Kawauchi N, Minami M. Mucin-hypersecreting intrahepatic biliary neoplasms. *Radiology* 1988; **168**: 609-614

5 **Kim HJ**, Kim MH, Lee SK, Yoo KS, Park ET, Lim BC, Park HJ, Myung SJ, Seo DW, Min YI. Mucin-hypersecreting bile duct tumor characterized by a striking homology with an intraductal papillary mucinous tumor (IPMT) of the pancreas. *Endoscopy* 2000; **32**: 389-393

6 **Shibahara H**, Tamada S, Goto M, Oda K, Nagino M, Nagasaka T, Batra SK, Hollingsworth MA, Imai K, Nimura Y, Yonezawa S. Pathologic features of mucin-producing bile duct tumors: two histopathologic categories as counterparts of pancreatic intraductal papillary-mucinous neoplasms. *Am J Surg Pathol* 2004; **28**: 327-338

7 **Zen Y**, Sasaki M, Fujii T, Chen TC, Chen MF, Yeh TS, Jan YY, Huang SF, Nimura Y, Nakanuma Y. Different expression patterns of mucin core proteins and cytokeratins during intrahepatic cholangiocarcinogenesis from biliary intraepithelial neoplasia and intraductal papillary neoplasm of the bile duct--an immunohistochemical study of 110 cases of hepatolithiasis. *J Hepatol* 2006; **44**: 350-358

8 **Furukawa T**, Klöppel G, Volkan Adsay N, Albores-Saavedra J, Fukushima N, Horii A, Hruban RH, Kato Y, Klimstra DS, Longnecker DS, Lüttges J, Offerhaus GJ, Shimizu M, Sunamura M, Suriawinata A, Takaori K, Yonezawa S. Classification of types of intraductal papillary-mucinous neoplasm of the pancreas: a consensus study. *Virchows Arch* 2005; **447**: 794-799

9 **Adsay NV**, Adair CF, Heffess CS, Klimstra DS. Intraductal oncocytic papillary neoplasms of the pancreas. *Am J Surg Pathol* 1996; **20**: 980-994

10 **Isaji S**, Kawarada Y, Taoka H, Tabata M, Suzuki H, Yokoi H. Clinicopathological features and outcome of hepatic resection for intrahepatic cholangiocarcinoma in Japan. *J Hepatobiliary Pancreat Surg* 1999; **6**: 108-116

11 **Helpap B**. Malignant papillomatosis of the intrahepatic bile ducts. *Acta Hepatogastroenterol (Stuttg)* 1977; **24**: 419-425

12 **Kim YI**, Yu ES, Kim ST. Intraductal variant of peripheral cholangiocarcinoma of the liver with Clonorchis sinensis infection. *Cancer* 1989; **63**: 1562-1566

13 **Taguchi J**, Yasunaga M, Kojiro M, Arita T, Nakayama T, Simokobe T. Intrahepatic and extrahepatic biliary papillomatosis. *Arch Pathol Lab Med* 1993; **117**: 944-947

14 **Yamaguchi H**, Shimizu M, Ban S, Koyama I, Hatori T, Fujita I, Yamamoto M, Kawamura S, Kobayashi M, Ishida K, Morikawa T, Motoi F, Unno M, Kanno A, Satoh K, Shimosegawa T, Orikasa H, Watanabe T, Nishimura K, Ebihara Y, Koike N, Furukawa T. Intraductal tubulopapillary neoplasms of the pancreas distinct from pancreatic intraepithelial neoplasia and intraductal papillary mucinous neoplasms. *Am J Surg Pathol* 2009; **33**: 1164-1172

15 **Nakayama Y**, Inoue H, Hamada Y, Takeshita M, Iwasaki H, Maeshiro K, Iwanaga S, Tani H, Ryu S, Yasunami Y, Ikeda S. Intraductal tubular adenoma of the pancreas, pyloric gland type: a clinicopathologic and immunohistochemical study of 6 cases. *Am J Surg Pathol* 2005; **29**: 607-616

16 **Zen Y**, Fujii T, Itatsu K, Nakamura K, Minato H, Kasashima S, Kurumaya H, Katayanagi K, Kawashima A, Masuda S, Niwa H, Mitsui T, Asada Y, Miura S, Ohta T, Nakanuma Y. Biliary papillary tumors share pathological features with intraductal papillary mucinous neoplasm of the pancreas. *Hepatology* 2006; **44**: 1333-1343

17 **Zen Y**, Fujii T, Itatsu K, Nakamura K, Konishi F, Masuda S, Mitsui T, Asada Y, Miura S, Miyayama S, Uehara T, Katsuyama T, Ohta T, Minato H, Nakanuma Y. Biliary cystic tumors with bile duct communication: a cystic variant of intraductal papillary neoplasm of the bile duct. *Mod Pathol* 2006; **19**: 1243-1254

18 **Devaney K**, Goodman ZD, Ishak KG. Hepatobiliary cystadenoma and cystadenocarcinoma. A light microscopic and immunohistochemical study of 70 patients. *Am J Surg Pathol* 1994; **18**: 1078-1091

19 **Albores-Saavedra J**, Sheahan K, O'Riain C, Shukla D. Intraductal tubular adenoma, pyloric type, of the pancreas: ad-

ditional observations on a new type of pancreatic neoplasm. *Am J Surg Pathol* 2004; **28**: 233-238
20 **Kato N**, Akiyama S, Motoyama T. Pyloric gland-type tubular adenoma superimposed on intraductal papillary mucinous tumor of the pancreas. Pyloric gland adenoma of the pancreas. *Virchows Arch* 2002; **440**: 205-208
21 **Bakotic BW**, Robinson MJ, Sturm PD, Hruban RH, Offerhaus GJ, Albores-Saavedra J. Pyloric gland adenoma of the main pancreatic duct. *Am J Surg Pathol* 1999; **23**: 227-231
22 **Oh DK**, Kim SH, Choi SH, Jang KT. Intraductal tubular carcinoma of the pancreas: a case report with the imaging findings. *Korean J Radiol* 2008; **9**: 473-476
23 **Itatsu K**, Sano T, Hiraoka N, Ojima H, Takahashi Y, Sakamoto Y, Shimada K, Kosuge T. Intraductal tubular carcinoma in an adenoma of the main pancreatic duct of the pancreas head. *J Gastroenterol* 2006; **41**: 702-705
24 **Shahinian HK**, Sciadini MF, Springer DJ, Reynolds VH, Lennington WJ. Tubular adenoma of the main pancreatic duct. *Arch Surg* 1992; **127**: 1254-1255
25 **Sato Y**, Osaka H, Harada K, Sasaki M, Nakanuma Y. Intraductal tubular neoplasm of the common bile duct. *Pathol Int* 2010; **60**: 516-519
26 **Nakanuma Y**, Sato Y, Harada K, Sasaki M, Xu J, Ikeda H. Pathological classification of intrahepatic cholangiocarcinoma based on a new concept. *World J Hepatol* 2010; **2**: 419-427
27 **Tsutsumida H**, Swanson BJ, Singh PK, Caffrey TC, Kitajima S, Goto M, Yonezawa S, Hollingsworth MA. RNA interference suppression of MUC1 reduces the growth rate and metastatic phenotype of human pancreatic cancer cells. *Clin Cancer Res* 2006; **12**: 2976-2987
28 **Park SY**, Roh SJ, Kim YN, Kim SZ, Park HS, Jang KY, Chung MJ, Kang MJ, Lee DG, Moon WS. Expression of MUC1, MUC2, MUC5AC and MUC6 in cholangiocarcinoma: prognostic impact. *Oncol Rep* 2009; **22**: 649-657
29 **Gumbiner BM**. Signal transduction of beta-catenin. *Curr Opin Cell Biol* 1995; **7**: 634-640
30 **Kiesslich T**, Alinger B, Wolkersdörfer GW, Ocker M, Neureiter D, Berr F. Active Wnt signalling is associated with low differentiation and high proliferation in human biliary tract cancer in vitro and in vivo and is sensitive to pharmacological inhibition. *Int J Oncol* 2010; **36**: 49-58
31 **Sugimachi K**, Taguchi K, Aishima S, Tanaka S, Shimada M, Kajiyama K, Sugimachi K, Tsuneyoshi M. Altered expression of beta-catenin without genetic mutation in intrahepatic cholangiocarcinoma. *Mod Pathol* 2001; **14**: 900-905
32 **Itatsu K**, Zen Y, Ohira S, Ishikawa A, Sato Y, Harada K, Ikeda H, Sasaki M, Nimura Y, Nakanuma Y. Immunohistochemical analysis of the progression of flat and papillary preneoplastic lesions in intrahepatic cholangiocarcinogenesis in hepatolithiasis. *Liver Int* 2007; **27**: 1174-1184
33 **Abraham SC**, Lee JH, Hruban RH, Argani P, Furth EE, Wu TT. Molecular and immunohistochemical analysis of intraductal papillary neoplasms of the biliary tract. *Hum Pathol* 2003; **34**: 902-910

S- Editor Gou SX **L- Editor** Kerr C **E- Editor** Zhang DN

HEPATOLOGY
Official Journal of the American Association for the Study of Liver Diseases

Histological Diversity in Cholangiocellular Carcinoma Reflects the Different Cholangiocyte Phenotypes

Mina Komuta,[1] Olivier Govaere,[1] Vincent Vandecaveye,[2] Jun Akiba,[3] Werner Van Steenbergen,[4] Chris Verslype,[4] Wim Laleman,[4] Jacques Pirenne,[5] Raymond Aerts,[6] Hirohisa Yano,[3] Frederik Nevens,[4] Baki Topal,[6] and Tania Roskams[1]

Cholangiocellular carcinoma (CC) originates from topographically heterogeneous cholangiocytes. The cylindrical mucin-producing cholangiocytes are located in large bile ducts and the cuboidal non–mucin-producing cholangiocytes are located in ductules containing bipotential hepatic progenitor cells (HPCs). We investigated the clinicopathological and molecular features of 85 resected CCs (14 hilar CCs [so-called Klatskin tumor], 71 intrahepatic CCs [ICCs] including 20 cholangiolocellular carcinomas [CLCs], which are thought to originate from HPCs]) and compared these with the different cholangiocyte phenotypes, including HPCs. Immunohistochemistry was performed with biliary/HPC and hepatocytic markers. Gene expression profiling was performed in different tumors and compared with nonneoplastic different cholangiocyte phenotypes obtained by laser microdissection. Invasion and cell proliferation assay were assessed using different types of CC cell lines: KMC-1, KMCH-1, and KMCH-2. Among 51 ICCs, 31 (60.8%) contained only mucin-producing CC features (muc-ICCs), whereas 39.2% displayed histological diversity: focal hepatocytic differentiation and ductular areas (mixed-ICCs). Clinicopathologically, muc-ICCs and hilar CCs showed a predominantly (peri-)hilar location, smaller tumor size, and more lymphatic and perineural invasion compared with mixed-ICCs and CLCs (predominantly peripheral location, larger tumor size, and less lymphatic and perineural invasion). Immunoreactivity was similar in muc-ICCs and hilar CCs and in mixed-ICCs and CLCs. *S100P* and *MUC1* were significantly up-regulated in hilar CCs and muc-ICCs compared with mixed-ICCs and CLCs, whereas *NCAM1* and *ALB* tended to be up-regulated in mixed-ICCs and CLCs compared with other tumors. KMC-1 showed significantly higher invasiveness than KMCH-1 and KMCH-2. *Conclusion:* Muc-ICCs had a clinicopathological, immunohistochemical, and molecular profile similar to that of hilar CCs (from mucin-producing cholangiocytes), whereas mixed-ICCs had a profile similar to that of CLCs (thought to be of HPC origin), possibly reflecting their respective cells of origin. (HEPATOLOGY 2012;55:1876-1888)

Cholangiocellular carcinoma (CC) is a primary liver tumor originating from cholangiocytes (epithelial cells that line the bile duct). Cholangiocytes are topographically heterogeneous within the different levels of the biliary tree.[1] The biliary tree is divided anatomically into extra- and intrahepatic bile duct (BD). Hilar BD and right and left hepatic BD are considered extrahepatic BD, and they are lined by cylindrical mucin-producing cholangiocytes. Inside the liver, a large intrahepatic BD (such as segmental, area, and septal BD) has a lining of similar mucin-producing cylindrical cells, whereas a small intrahepatic BD (such as interlobular BD and ductules) is lined with mucin-negative cuboidal cholangiocytes. In addition, ductules contain hepatic progenitor cells (HPCs),[2] which can differentiate into both hepatocytes

Abbreviations: ANXA3, annexin A3; BD, bile duct; CC, cholangiocellular carcinoma; CLC, cholangiolocellular carcinoma; DR, ductular reaction; EMA, epithelial membrane antigen; EpCAM, epithelial cell adhesion molecule; HCC, hepatocellular carcinoma; hep-dif, hepatocytic differentiation; HPC, hepatic progenitor cell; ICC, intrahepatic CC; mixed-ICC, ICC with mixed features; MRI, magnetic resonance imaging; muc-ICC, mucin-producing ICC; NCAM, neural cell adhesion molecule; pCEA, polyclonal carcinoembryonic antigen; PSC, primary sclerosing cholangitis; RT-PCR, reverse-transcription polymerase chain reaction; TACSTD2, tumor-associated calcium signal transducer 2; WHO, World Health Organization.

From the Departments of [1]Morphology and Molecular Pathology, [2]Radiology, [4]Hepatology, [5]Abdominal Transplant Surgery, and [6]Abdominal Surgery, University Hospitals Leuven, Leuven, Belgium; and the [3]Department of Pathology, Kurume University School of Medicine, Fukuoka, Japan

Received July 30, 2011; accepted December 23, 2011.

Supported by an Interuniversity Attraction Pole (IUAP) grant from Belspo Belgium.

and cholangiocytes and can give rise to tumors during the differentiation process.[3] HPC-derived tumors can display varying hepatocytic and/or cholangiocytic differentiation characteristics within the same tumor. For example, cholangiolocellular carcinoma (CLC), a subtype of intrahepatic CC (ICC), is reported as an HPC-derived tumor showing histological diversity with hepatocytic and/or cholangiocytic differentiation characteristics.[4] Therefore, we hypothesized that the different cholangiocyte phenotypes could lead to different clinicopathological phenotypes of CC. Mucin-producing cylindrical cholangiocytes could lead to mucin-producing CC such as hilar CC (Klatskin tumor), whereas mucin-negative cuboidal cholangiocytes, including HPCs, could give rise to tumors with histological variation, such as hepatocytic and cholangiocytic differentiation characteristics (as in CLC).

World Health Organization (WHO) classification is based on the original location (BD) of the tumor.[5] CC arising from the right and left hepatic ducts, at or near their junction, is called hilar CC (Klatskin tumor) and is considered an extrahepatic lesion. CC arising from the intrahepatic large BDs (intrahepatic second branches or segmental branches) is called peri-hilar ICC and is considered an intrahepatic lesion.[5] We anticipate that hilar CC and peri-hilar ICC could have a similar tumor profile, because they arise from similar mucin-producing cholangiocytes. In addition, liver hilum is a location of hilar CC and peri-hilar CC, because large BD locates mainly in the liver hilum. However, the biliary system inside the liver has a three-dimensional tree-like structure, harboring small ducts in the hilar as well as in the peripheral subcapsular regions. Therefore, liver hilum has the potential to contain an HPC-derived ICC that shows histological diversity, as well as peri-hilar CC. We hypothesize that different CC phenotypes may reflect the cholangiocyte phenotype and can thus resolve the issues of the current anatomical-based classification of CC.[5,6] As the recent incidence and associated mortality of CC has been increasing, the need for a review of the current anatomical-based classification has become evident. The current classification system does not allow accurate assessment of epidemiological background and patient outcome with CC.

We investigated 85 CCs, including 14 hilar CCs and 20 CLCs, and compared their clinicopathological features with the different nonneoplastic cholangiocytes. We correlated the immunohistochemistry and gene expression profiling of the nonneoplastic cholangiocytes with clinicopathological characteristics of the different CCs.

Patients and Methods

Patient Selection. We examined 85 consecutively resected CCs between 1991 and June 2011 (46 men, 39 women; mean age, 63.3 years) comprising 83 surgical resections and two explant livers. CCs were diagnosed by clinical and radiological data and confirmed with histological examination. The histological diagnosis was made according to WHO criteria.[5] The tumor staging was made according to 7th edition of the American Joint Committee on Cancer/Union for international Cancer Control TNM classification.[6] The specimens were treated and investigated as described.[4] Tumor location was classified based on surgical findings, macroscopic examination, and imaging studies, including computed tomography, magnetic resonance imaging (MRI), and endoscopic retrograde cholangiopancreaticography, when available.[5,7] Macroscopic type of ICCs was investigated according to the Liver Cancer Study Group of Japan.[8] This study was approved by the Local Commission for Medical Ethics.

Immunohistochemistry. Immunohistochemistry was performed on paraffin-embedded sections using a large BD marker (S100P)[9] epithelial membrane antigen (EMA, MUC1), HPC/biliary markers (K7, K19, neural cell adhesion molecule [NCAM],[10] tumor-associated calcium signal transducer 2 [TACSTD2, TROP2],[11] epithelial cell adhesion molecule [EpCAM, TACSTD1, TROP1],[12] and annexin A3 [ANXA3][13]), and hepatocytic markers (Hep Par 1, and canalicular polyclonal carcinoembryonic antigen [pCEA]) (Supporting File 1). The slides were reviewed by two independent pathologists (M. Komuta and T. Roskams). Immunoreactivity was considered positive if more than 1% of tumor cells were stained in the proper pattern. TACSTD2 overexpression was scored as described before.[14]

Address reprint requests to: Mina Komuta, M.D., Laboratory of Morphology and Molecular Pathology, Minderbroederstraat 12, 3000 Leuven, Belgium. E-mail: mina.komuta@gmail.com; fax: (32)-16-336548.

View this article online at wileyonlinelibrary.com.
DOI 10.1002/hep.25595
Potential conflict of interest: Nothing to report.
Additional Supporting Information may be found in the online version of this article.

Real-Time Quantitative Reverse-Transcription Polymerase Chain Reaction of Tumor Samples. Five hilar CCs, six mucin-producing ICCs (muc-ICCs), seven ICCs with mixed features (mixed-ICCs), and seven CLCs were included for reverse-transcription polymerase chain reaction (RT-PCR) analysis for the following genes: *KRT19/7, ANXA3, TACSTD2, EpCAM, NCAM1, ALB, S100P,* and *MUC1.* Sequences and a detailed protocol are listed in Supporting File 2.

Invasion Assay and Cell Proliferation Assay Using Cell Lines. Three different human CC cell lines, KMC-1, KMCH-1, and KMCH-2, which were originally established at the Department of Pathology, Kurume University School of Medicine, were used. KMC-1 was established from an intrahepatic-CC observed as a tubular adenocarcinoma with mucin production.[15] KMCH-1 was established from a combined hepatocellular-cholangiocarcinoma comprising both a hepatocellular carcinoma (HCC) area and a CC area.[16] KMCH-2 was established from a combined hepatocellular cholangiocarcinoma showing intermediate features between HCC and CC.[17] These cell lines were previously confirmed to retain the morphological and functional characteristics of the original tumor. The invasive ability *in vitro* was measured by using BD BioCoat Matrigel Invasion Chambers (BD Bioscience, Bedford, MA). The growth of cultured cells was examined with colorimetry using the MTT assay kit (Chemicon International Inc., Temecula, CA). Further information is provided in Supporting File 3.

Microdissection of Hilar BD, Segmental BD, and Ductular Reaction. Human liver specimens from liver explants and resections taken for diagnostic purposes were used in this study, including hilar BD lined with mucin-secreting cholangiocytes (n = 6) and segmental BD lined with mucin-secreting cholangiocytes (n = 4) which were obtained from normal looking hilar and segmental BDs at a distance of a benign tumor, and activated HPCs/ductular reaction (DR) (n = 8) obtained from HCV-related chronic hepatitis (n = 4) and primary sclerosing cholangitis (PSC)-related chronic biliary disease (n = 4). Tissue samples were obtained using the laser capture microdissection LMD6500 system (Leica Microsystems, Wetzlar, Germany). Further information is provided in Supporting File 4.

Preoperative MRI. Forty-six MRI studies were available for evaluation and reviewed by an expert abdominal radiologist in a blinded manner. Further information is provided in Supporting File 5.

Clinical Outcome. Nine of the 85 patients were excluded from survival analysis for the following reasons: two patients were lost to follow-up, and seven patients died in hospital from liver failure, multiple organ failure, or bleeding. Thus, 76 patients were ultimately analyzed for survival and outcome. Overall survival was defined as the interval between treatment and death, or the date of the last or most recent follow-up. Recurrence-free survival was defined as the interval between treatment and the date of recurrence, which was monitored by clinical and imaging assessment, until the patient's death, or the end of the study. Survival curves were computed according to the Kaplan-Meier method and compared using the log-rank test.

Statistical Analysis. Continuous data are expressed as the mean ± SD. Detection of significances between the four groups was done using chi-square and Kruskal-Wallis analysis of variance for categorical and continuous data, respectively. Post hoc comparisons between groups were performed using chi-square and Mann-Whitney U tests, with Bonferroni correction for multiple testing. Analysis was performed using GraphPad Prism software (GraphPad Software, Inc., CA). $P < 0.05$ was considered statistically significant.

Results

Histopathological Variation in Hilar CCs, Intrahepatic CCs, and CLCs. Using the WHO classification, 85 CCs were classified into 14 (16.5%) hilar CCs and 71 (83.5%) intrahepatic CCs (ICCs) (Fig. 1). Among the 71 intrahepatic ICCs, 20 (28.2%) were diagnosed as CLCs.[4] Of the remaining 51 ICCs, 31 (60.8%) comprised pure mucin-producing adenocarcinomas (muc-ICCs), and the other 20 (39.2%) exhibited features of predominant mucin-producing adenocarcinoma with histological diversity (hepatocytic differentiation areas [hep-dif] and/or ductular areas in the tumor [mixed-ICC]). A hep-dif area was defined as a thick trabecular and/or solid growth pattern with little stroma, and tumor cells with abundant eosinophilic cytoplasm, mild atypia, and no mucin production. Hepatocytic differentiation (hep-dif) areas were always located at the tumor boundary, proliferating as if it was replacing the surrounding liver cell cords, and associated with lymphoid infiltration. A ductular area was characterized by ductular reaction-like anastomosing glands in edematous fine fibrous stroma with mild atypia, no mucin production, and cuboidal tumor cells. In contrast with hep-dif areas, ductular areas and mucin-producing adenocarcinoma were mainly seen in the center of the tumor with abundant fibrous stroma. This histological diversity, which was seen in mixed-

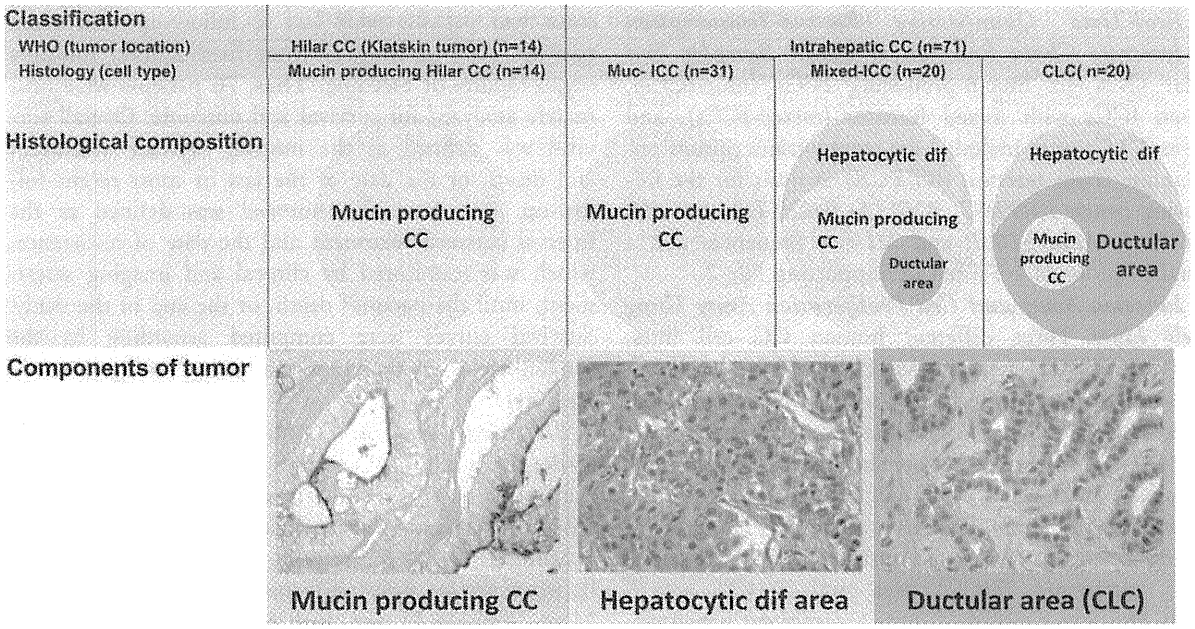

Fig. 1. Histological variation of 14 hilar CCs and 71 ICCs, including 20 CLCs. All hilar CCs and 31 ICCs (muc-ICCs) showed only mucin-positive CCs, whereas 20 mixed-ICCs and 20 CLCs contained mixed histological features (hepatocytic differentiated areas and/or ductular areas).

ICCs, has been already described in CLCs.[4] Thus, mixed-ICC and CLC have overlapping histopathological aspects. Ductular areas have been described as a typical feature of CLC.[4] The only difference between mixed-ICC and CLC was the predominant feature: where CLC showed ductular areas in more than 90% of the tumor, mixed-ICCs showed predominant mucin producing CC with focal hep-dif and/or ductular areas.

We further investigated the clinicopathological features and gene expression profiling of 14 hilar CCs, 31 muc-ICCs, 20 mixed-ICCs and 20 CLCs (based on histological classification).

Clinicopathomorphological Findings in Hilar CCs, Muc-ICCs, Mixed-ICCs, and CLCs Etiology. The etiology of underlying liver disease is listed in Table 1. Although there were no significant differences, hepatitis B or C infection was seen mainly in mixed-ICCs and CLCs compared with hilar CCs and muc-ICCs, while PSC was seen primarily in muc-ICCs/hilar CCs.

Gross Findings. All hilar CCs were located in the liver hilum. About 77% of the muc-ICCs were located in the perihilar area, while 80% of the mixed-ICCs and 75% CLCs were located in the peripheral area ($P < 0.05$). All mixed-ICCs and CLCs showed a mass forming growth pattern, while muc-ICCs showed both a mass-forming growth pattern and a combination of a mass-forming growth pattern with a periductal infiltrative growth pattern. All hilar CCs and more than 90% of muc-ICCs were a single tumor, whereas around 20% of mixed-ICCs and CLCs were multiple tumors. Tumor size was significantly smaller in hilar CCs and muc-ICCs compared with mixed-ICCs and CLCs. All 85 CCs underwent surgery with curative intent. Positive microscopic resection margin was seen in two (14.3%) hilar CCs, six (19.4%) muc-ICCs, one (5%) mixed-ICC, and two (10%) CLCs.

Histological Findings. All hilar CCs and 27 (87.1%) muc-ICCs showed secondary cholangitis associated with parenchymal necrosis/inflammation. Bile duct dysplasia in surrounding nontumoral liver tissue was significantly seen in hilar CCs compared with mixed-ICCs and CLCs. Hilar CCs and muc-ICCs showed mucin-producing adenocarcinoma of predominantly well to moderate differentiation. On the other hand, mixed-ICCs and CLCs could not be categorized based on tumor differentiation because of their histological diversity. Lymphatic and perineural invasion were significantly higher in hilar CCs and muc-ICCs compared with mixed-ICCs and CLCs. Hilar CCs and muc-ICCs showed similar histopathological aspects, whereas CLCs and mixed-ICCs were histologically overlapping.

These different cancer areas correlated with the different types and amount of stroma (Supporting Fig.1).

Table 1. Clinicopathological Features of Hilar CC and ICC

WHO Classification	Hilar CC (Klatskin Tumor; n = 14)	ICC (n = 71)			
Histological Classification	Hilar CC (n = 14)	Muc-ICC (n = 31)	Mixed-ICC (n = 20)	CLC (n = 20)	*P* Value
Age, years, range (mean ± SD)	40-77 (59.1 ± 10.6)	26-85 (62.9 ± 14.4)	50-84 (64.1 ± 9.9)	48-79 (64.2 ± 8.8)	0.9831
Sex, male/female	9/5	17/14	12/8	8/12	0.4801
Etiology					
HBsAg- or HCVAB-positive	1 (7.1)	1 (3.2)	3 (15.0)	2 (10.0)	
PSC	1 (7.1)	4 (13.0)	1 (5.0)	0 (0)	
(Non-)alcoholic steatohepatitis	0 (0)	1 (3.2)	2 (10.0)	3 (15.0)	
Other	0 (0)	0 (0)	1[§] (5.0)	2[‖] (10.0)	
No underlying liver disease	12 (85.8)	25 (80.6)	13 (65.0)	13 (65.0)	
Tumor location (WHO)*					<0.0001
Hilar (extrahepatic)	14 (100)	0 (0)	0 (0)	0 (0)	
Perihilar (intrahepatic)	0 (0)	24 (77.4)	4 (20.0)	5 (25.0)	
Periphery (intrahepatic)	0 (0)	7 (22.6)	16 (80.0)	15 (75.0)	
Stage (AJCC/UICC)†					
I	0	3 (9.7)	6 (30.0)	3 (15.0)	
II	11[†]	14 (45.2)	11 (55.0)	11 (55.0)	
III	3 (IIIB)[†]	2 (6.4)	0	3 (15.0)	
IVa	0	12 (38.7)	3 (15.0)	3 (15.0)	
Macroscopic finding					
MF		14	20	20	
PI		0	0	0	
IG		2	0	0	
MF+PI		13	0	0	
MF+IG		2	0	0	
Number of nodules					0.0819
1	14 (100)	29 (93.5)	15 (75.0)	16 (80.0)	
≥2	0 (0)	2 (6.5)	5 (25.0)	4 (20.0)	
Tumor size (mm)					<0.0001
Range (mean ± SD)	10-40 (23.1 ± 9.2)	8-120 (41.2 ± 26.2)	20-125 (67.3 ± 28.6)	20-170 (64.6 ± 35.2)	
<20	7	5	1	1	
21-30	5	11	2	1	
31-40	2	5	1	2	
41-50	0	3	3	7	
≥50	0	7	13	9	
Histological findings					
BD dysplasia‡	8 (57.1)	10 (32.3)	3 (15)	2 (10.0)	0.0104
Vascular invasion	10 (71.4)	26 (83.9)	12 (60.0)	15 (75.0)	0.2986
Lymphatic invasion	13 (92.9)	27 (87.1)	12 (60.0)	9 (45.0)	0.0017
Perineural invasion	13 (92.9)	25 (80.7)	9 (45.0)	10 (50.0)	0.0031
Lymph node involvement	3/13 (23.1)	12/22 (54.5)	3/12 (25.0)	3/14 (21.4)	0.1020
Immunohistochemistry					
S100P-positive	14 (100)	30 (96.8)	0 (0)	0 (0)	<0.0001
TACSTD2 overexpression	11 (78.6)	30 (96.8)	10 (50.0)	8 (40.0)	<0.0001

Abbreviations: AJCC/UICC, American Joint Cancer Committee/Union Internationale Contrele-Cancer; HBsAg, hepatitis B surface antigen; HCVAB, hepatitis C virus IG, intraductal growth; MF, mass-forming; PI, periductal infiltrative.

Data are presented as no. (%) unless indicated otherwise.

*Tumor location was defined by WHO classification.

†Hilar CC was staged according to extrahepatic BD cancer classification; the others were staged according to intrahepatic BD cancer classification.

‡BD dysplasia in the surrounding nontumoral liver tissue.

§Hemochromatose (n = 1).

‖Hemochromatose (n = 1), α1-antitrypsin-deficient (n = 1).

Hep-dif areas contained a small amount of fine fibrosis located around the tumor nests and were associated with lymphocytic inflammation and narrow blood spaces. In contrast, mucin-producing CC areas showed hyalinizing, abundant, dense fibrous stroma occupying around 40%-50% of the area. Lymphocytic infiltration in the stroma became more prominent in cases of BD obstruction, which gave rise to abscess formation and lymphocyte infiltration associated with lymphoid follicles. Ductular areas showed mainly edematous fibrous stroma accompanied by lymphocytic infiltration that occupied approximately 30%-50% of the area. Hep-dif areas and ductular areas were seen in varying degree in the tumor, and they showed transitional zones between each other and with the mucin-producing adenocarcinoma area.

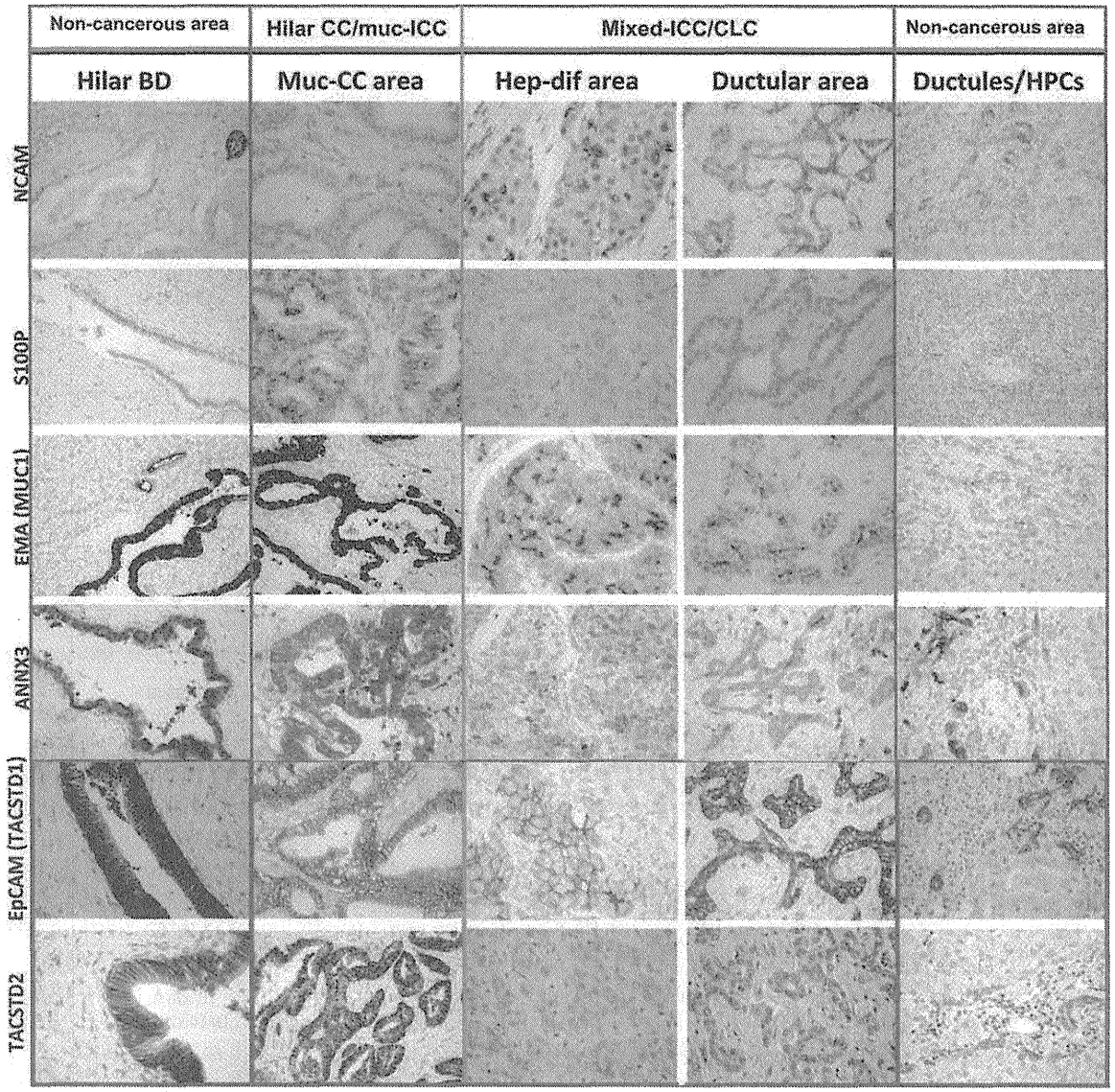

Fig. 2. Immunohistochemical profiles in different tumor types compared with different levels of the BD. Mucin-producing CC area in hilar CCs and muc-ICCs showed similar immunohistochemical profiles to hilar BD, which showed cytoplasmic/nuclear positivity for S100P and intense cytoplasmic positivity for EMA, ANNX3, EpCAM, and TACSTD2, and no positivity for NCAM. Ductular areas in mixed-ICCs and CLCs showed a similar immunohistochemical profile to ductules/HPCs with membranous positivity for NCAM, cytoplasmic positivity for ANNX3, EpCAM, and TACSTD2, and apical positivity for EMA. Hep-dif showed focal positivity for NCAM, ANNX3, and TACSTD2, membranous positivity for EpCAM, and canalicular-like/cytoplasmic positivity for EMA. S100P expression was negative in the hep-dif and ductular areas.

Immunohistochemical Profiles of Different Tumors (Hilar CCs, Muc-ICCs, Mixed-ICCs, and CLCs) Compared with Normal Counterparts (Hilar BD and Ductules/ HPCs). Mucin-positive CC areas in hilar CCs and muc-ICCs showed similar immunohistochemical staining patterns to hilar BD, with cytoplasmic/nuclear positivity for S100P, intense cytoplasmic positivity for EMA, ANNX3, EpCAM, and TACSTD2, and no positivity for NCAM (Fig. 2). Mucin-positive CC areas (n = 30) in mixed-ICCs and CLCs showed similar immunoprofiles to those areas from hilar CCs and muc-ICCs, apart from S100P immunoreactivity. S100P expression was seen only in mucin-positive CC areas in hilar CCs and muc-ICCs, but not in the mixed-ICCs and CLCs.

Ductular areas in mixed-ICCs and CLCs showed similar immunohistochemical profiles to ductules/ HPCs; they demonstrated membranous positivity for

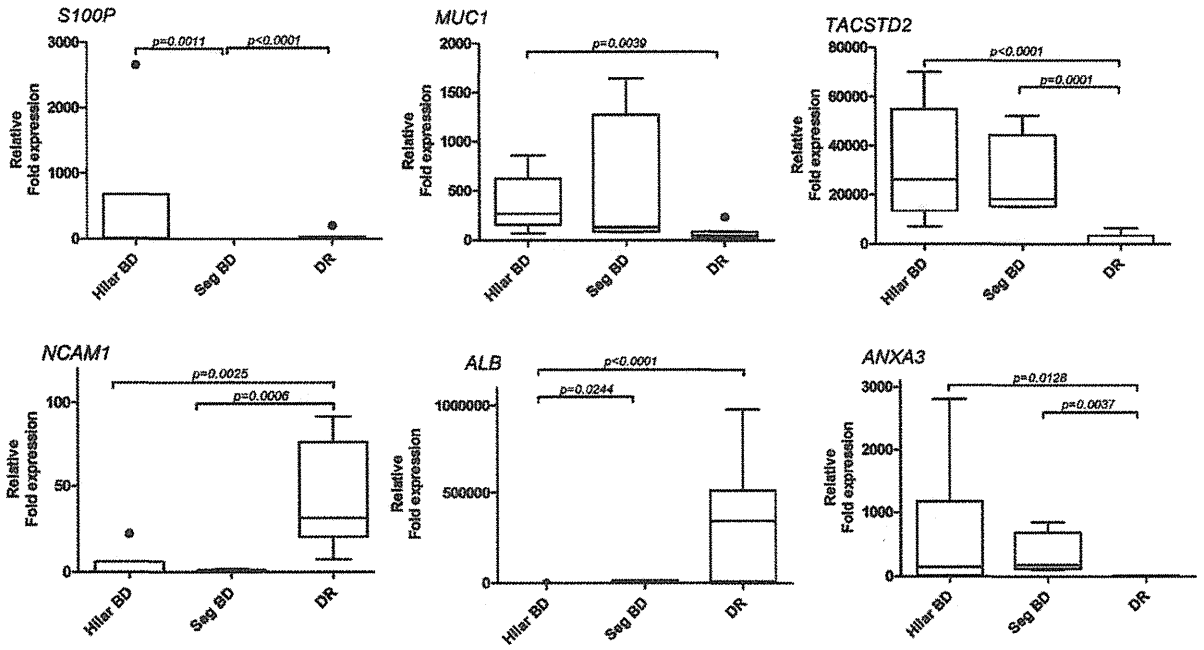

Fig. 3. Gene expression profiling. Box plots of RT-PCR results for biliary markers (*S100P* and *MUC1*), HPC/biliary markers (*NCAM1*, *ANXA3*, and *TACSTD2*), and hepatocytic marker *ALB* (hilar BD, n = 6; segmental BD, n = 4; DR, n = 8).

NCAM, cytoplasmic positivity for ANNX3, EpCAM, and TACSTD2, and apical positivity for EMA. S100P was negative in both the ductular areas of mixed-ICCs and CLCs and ductules/HPCs.

Hep-dif areas showed focal positivity for NCAM, ANNX3, and TACSTD2, membranous positivity for EpCAM, a canalicular/abberrant canalicular pattern for pCEA, and canalicular-like/cytoplasmic positivity for EMA in mixed-ICCs and CLCs. Focal Hep Par 1 expression was seen in 11 (55%) mixed-ICCs and 16 (80%) CLCs. S100P expression was negative in the hep-dif area.

Gene Expression Profiling of Hilar CCs, Muc-ICCs, Mixed-ICC, and CLCs Compared with Different Levels of BD. We investigated six hilar BDs, four segmental BDs, and eight DRs obtained using laser capture microdissection (Fig. 3, Supporting Fig.2). *TACSTD2* and *ANXA3* showed significantly higher expression in hilar and segmental BD compared with DR, whereas *NCAM1* was significantly higher in DR compared with hilar and segmental BD. *MUC1* was significantly stronger in hilar BD compared with DR, whereas *ALB* showed significantly higher expression in DR compared with hilar BD. Among different levels of BD, hilar BD has more similar profiles with segmental BD compared with DR. For a comparison of different tumors, we investigated five hilar CCs, six muc-ICCs, seven mixed-ICCs, and seven CLCs (Fig. 4, Supporting Fig. 3). *S100P* and *MUC1* were significantly up-regulated in hilar CCs and muc-ICCs compared with mixed-ICCs and CLCs, whereas *NCAM1* and *ALB* tended to be up-regulated in mixed-ICCs and CLCs compared with other tumors. *KRT19* and *EpCAM* were significantly up-regulated in mixed-ICCs compared with hilar CCs, but their immunohistochemical expression (on protein level) was similar.

Invasion Assay and MTT Assay Using Cell Lines. The morphological features of KMC-1, KMCH-1, and KMCH-2 were identical to those described.[15-17] Based on the pathology of their original tumors, and cellular features of the cell line, KMC-1 was thought to correspond to muc-ICCs, and KMCH-1 and KMCH-2 were thought to be representative for the mixed-ICCs. KMC-1, corresponding to muc-ICCs, showed significantly higher invasiveness compared with KMCH-1 and KMCH-2 (corresponding to the mixed-ICCs) ($P < 0.01$) (Fig. 5). In contrast, KMCH-1 and KMCH-2 showed a significantly higher proliferation rate at 72 hours and 96 hours compared with KMC-1 ($P < 0.001$).

Preoperative MRI: Lesion Characteristics. Forty-six MRI studies correlated histologically with 8 hilar CCs, 14 muc-ICCs, 10 mixed-ICCs, and 14 CLCs. Hilar CCs presented as a small mass or enhancing biliary wall at the extrahepatic hepatic ducts and/or their bifurcation with the main BD. Detailed results for the

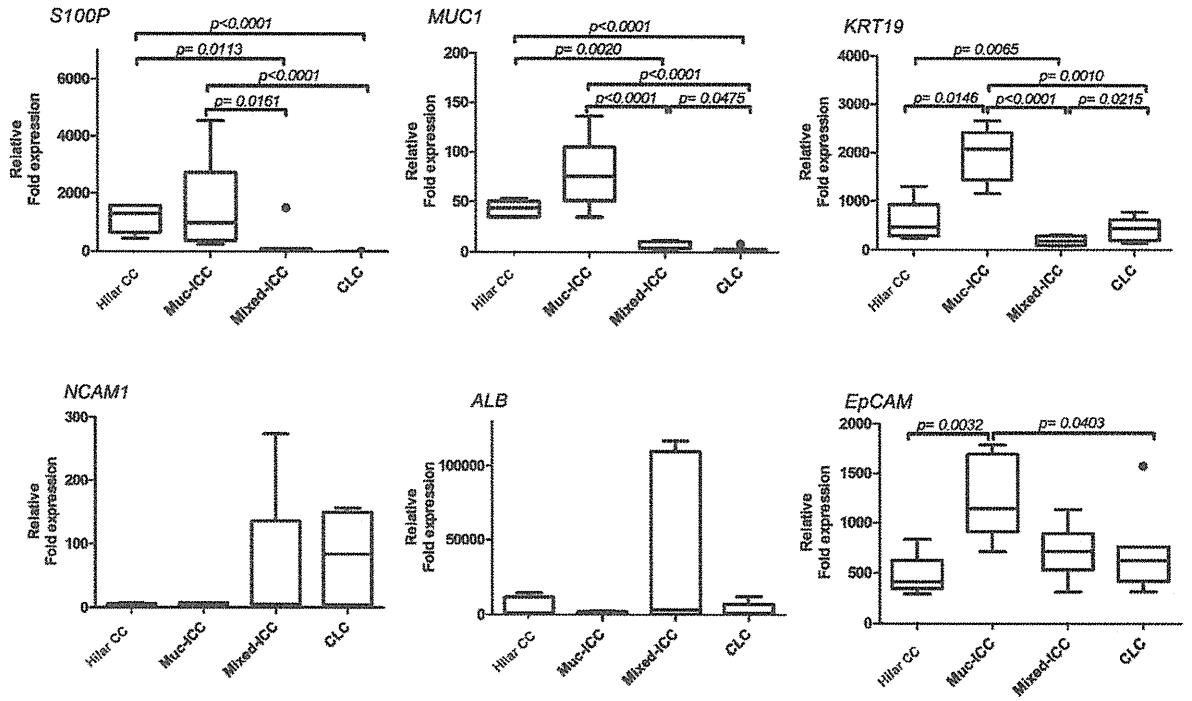

Fig. 4. Gene expression profiling. Box plots of RT-PCR results for HPC/biliary markers (*KRT19*, *NCAM1*, and *EpCAM*), biliary markers (*S100P* and *MUC1*), and hepatocytic marker *ALB* (hilar CCs, n = 5; muc-ICCs, n = 6; mixed-ICCs, n = 7; CLCs, n = 7).

intrahepatic tumors are summarized in Fig. 6. Briefly, all muc-ICCs showed homogeneous T2 intensity, whereas 70% of mixed-ICCs and 86% of CLCs showed mixed intensity, in concentric (peripheral hyperintense-central hypointense) or random nodular distribution. At dynamic contrast-enhanced imaging, all muc-ICCs showed concentric filling at venous phase, whereas mixed-ICCs/CLCs showed washout in various patterns. Historadiological comparison between muc-ICC and CLC is shown in Fig. 7.

Clinical and Follow-up Data. Seventy-six surgically treated patients (11 hilar CCs, 29 muc-ICCs, 18 mixed-ICCs, and 18 CLCs) were available for follow-up data (33-4,654 days, 833.3 ± 807.8). There was no statistically significant difference in recurrence-free survival days and overall survival days in these four groups. However, the hilar CC and muc-ICC groups tended to show worse prognosis compared with the mixed-ICC and CLC groups (Supporting Fig. 4).

Discussion

Cholangiocytes, which line the BDs, show topographic heterogeneity within the different levels of the biliary tree.[1] The heterogeneity of cholangiocytes is most distinct when comparing the smallest, mucin-negative cuboidal cholangiocytes located in the canal of Hering/ductules and the taller, cylindrical, mucin-producing cholangiocytes located in the larger BDs. The smallest cholangiocytes include hepatic progenitor cells (HPCs), which are able to differentiate into both hepatocytes and cholangiocytes. The taller cylindrical cholangiocytes show mucin production not seen in the small cholangiocytes. Currently, the anatomical-based tumor classification is often problematic due to the three-dimensional biliary structure and large tumor size. We hypothesized that CCs may reflect the heterogeneity of the cholangiocytes and that this may be useful for more precise tumor classification, as tumor histopathology reflects cellular origin. Therefore, we investigated the histological variation in ICCs and compared their different phenotypes with hilar CCs (so-called Klatskin tumor) and CLCs (thought to be originated from HPCs).

We were able to histopathologically categorize ICCs into two groups based on histological diversity; pure muc-ICC and mixed-ICC (mucin-producing adenocarcinoma with hepatocytic differentiation [hep-dif] areas and/or ductular areas). Muc-ICCs had similar clinicopathological, immunohistochemical, and gene expression profiles to hilar CCs, and the tumors had a similar profile to cylindrical, taller, mucin-producing cholangiocytes that line hilar and intrahepatic large BDs. In contrast, mixed-ICCs showed similar clinicopathological, immunohistochemical, and gene

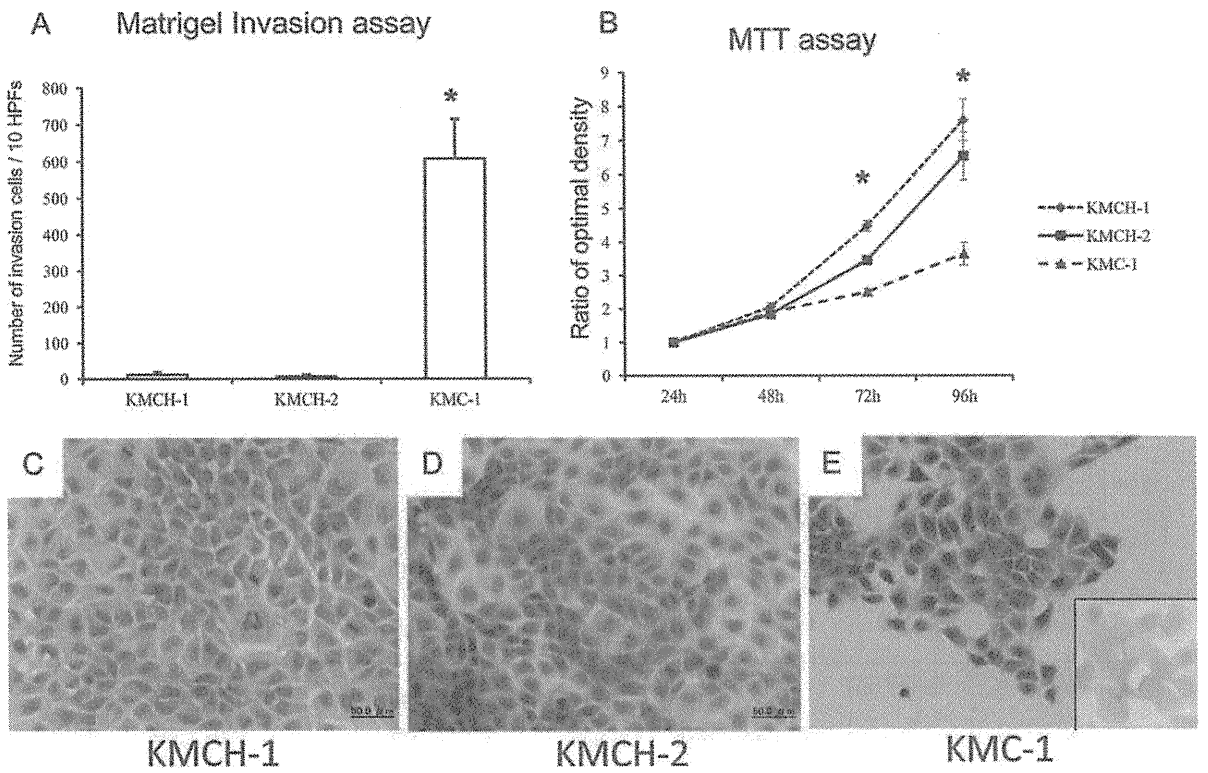

Fig. 5. Invasion and MTT assay. (A) KMC-1 showed significantly higher invasiveness compared with KMCH-1 and KMCH-2. *$P < 0.01$. (B) KMCH-1 and KMCH-2 cells showed a significantly faster proliferation rate at 72 hours and 96 hours compared with KMC-1. *$P < 0.001$. (C) KMCH-1 cells proliferated in pavestone arrangements, showing an abundant eosinophilic cytoplasm with a large, round nucleus containing distinct nucleoli. Some cells revealed cytoplasmic vacuoles. (D) KMCH-2 cells also proliferated with a pavestone arrangement. They comprised two different types of cells: large cells showing abundant eosinophilic cytoplasm with a round nucleus containing distinct nucleoli, and smaller cells with an increased nuclear/cytoplasmic ratio showing dark eosinophilic cytoplasm and oval-shaped, dense nuclei. (E) KMC-1 cells proliferated in a pavement-like monolayer pattern with a partly tubular formation. They had an irregular-shaped, medium to large cytoplasm with irregular-shaped, dark nuclei. Alcian blue-positive mucin was seen (inset).

expression profiles to CLCs (90% ductular areas with focal hep-dif areas and/or mucin-producing CC areas, which are thought to originate from HPCs). These tumors had similar profiles to mucin-negative cuboidal cholangiocytes that line the smallest BD (ductules). These features may indicate their different cells of origin; hilar CCs and muc-ICCs are from the hilar and large intrahepatic BD lined with mucin-producing cholangiocytes, while mixed-ICCs and CLCs are from the most peripheral biliary branches, ductules, which contain HPCs. In that respect, we think that mixed-ICCs and CLCs form part of a spectrum with combined hepatocellular-cholangiocarcinoma, which are also thought to be of possible HPC origin.[18-20]

Histological variation such as hep-dif and ductular areas could be indeed a sign of a HPC-related intrahepatic tumor. Because HPCs are able to differentiate into either hepatocytes or cholangiocytes, HPC-related tumors can display a whole spectrum of phenotypes with varying hepatocellular and cholangiocellular differentiation characteristics.[4,21] In addition, HPCs are located in the most peripheral biliary branches within the liver, so that histological diversity is not seen in the CC originating from the extrahepatic BD, as with hilar CCs. Recognizing these mixed features may be much easier by combining histopathology with immunohistochemistry of markers like NCAM and S100P. S100P, a member of the S100 family of EF-hand calcium-binding proteins,[22] was recently reported to be a useful diagnostic marker of ICC.[9,23] We showed S100P expression in hilar CCs and muc-ICCs only, but not in the mucin-producing adenocarcinoma component of mixed-ICCs. In contrast, NCAM, a marker of HPCs, was only immunoreactive in the hep-dif and ductular areas in mixed-ICCs and CLCs, but not in muc-ICCs and hilar CCs, as reported.[24] These mirror images are useful to distinguish muc-ICCs from mixed-ICCs and CLCs. Gene expression profiling in the different types of CCs showed significant differences in several genes. However, the differences of mRNA level

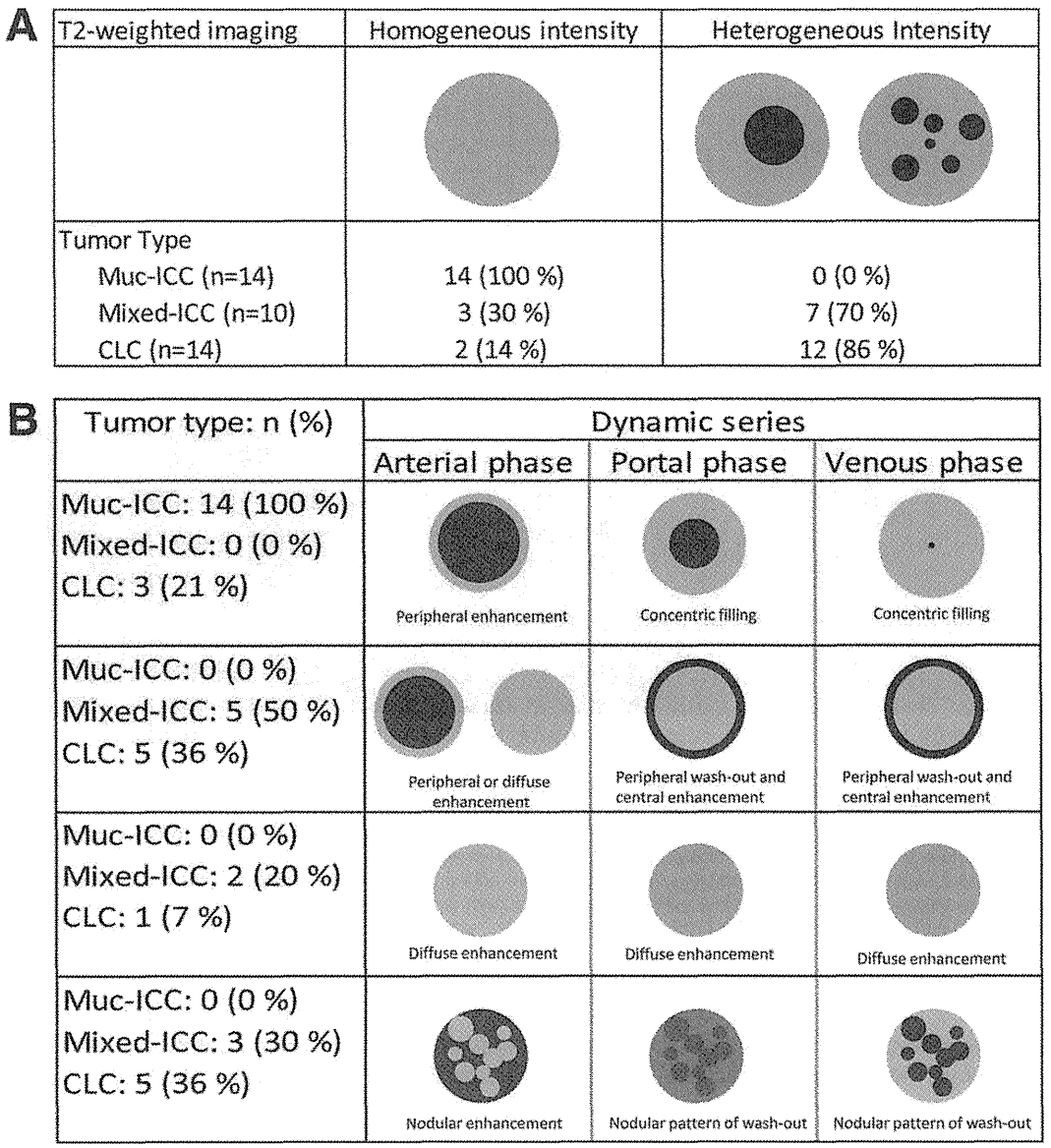

Fig. 6. Preoperative MRI: lesion characteristics. (A) Schematic representation of the different T2-weighted signal patterns in correlation to the tumor subtypes. (B) Schematic representation of the different contrast-enhancement patterns in correlation to the tumor subtypes.

assessment do not always correlate with the protein levels presented by immunohistochemistry. For instance, *KRT19* and *EpCAM* showed significant up-regulation in muc-ICCs compared with hilar CCs, although their immunoprofiles were exactly the same. Therefore, and for the usefulness of immunohistochemistry in clinical practice, S100P and NCAM are more useful markers.

The histological classification in this study was partially supported by tumor location. The mixed-ICCs and CLCs were mostly located in the periphery of the liver, which mainly comprises smaller BDs, whereas hilar CCs and muc-ICCs were mainly located in the liver hilum, which is predominantly composed of large BD. However, 20%-25% of mixed-ICCs and CLCs were located in the perihilar area, indicating the advantage of the histological-based classification over the anatomically based classification. The finer ramifications (ductules and canals of Hering) are also represented in the (peri-) hilar zones. This highlights the issue of the three-dimensional tree-like structure of the intrahepatic biliary system and the problems associated with the current anatomical-based classification. A

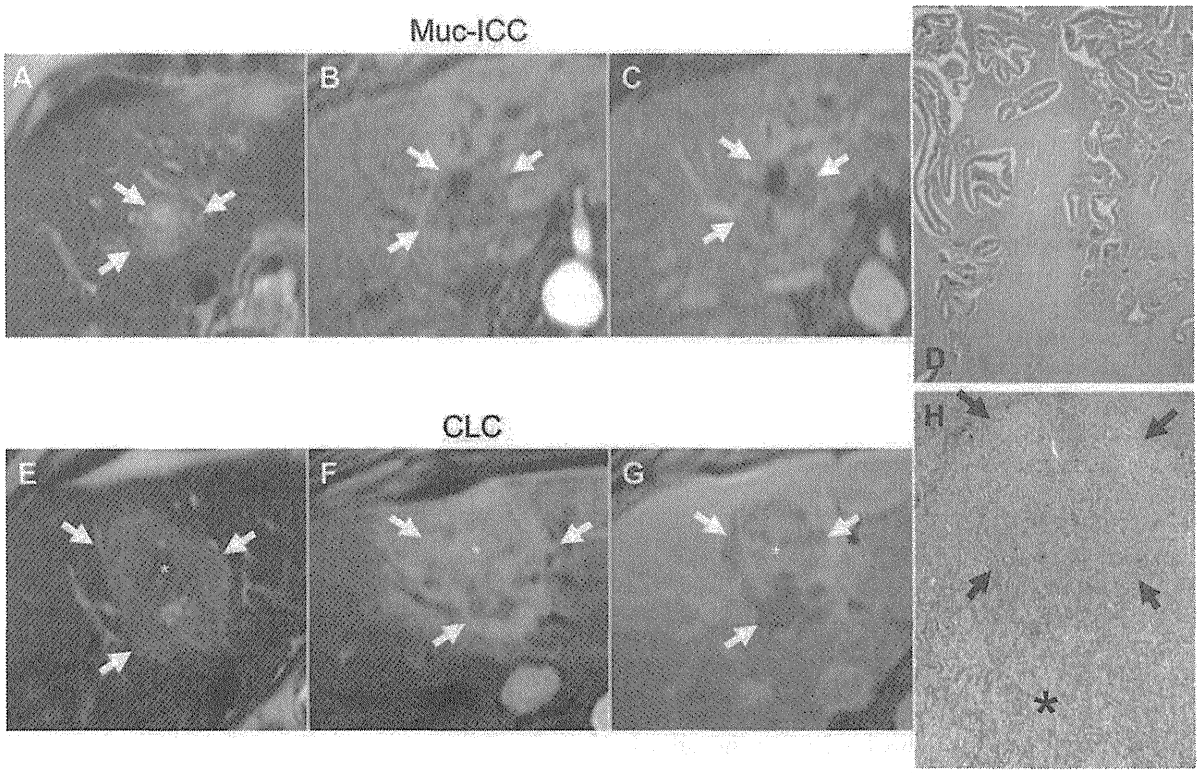

Fig. 7. Historadiological comparison between muc-ICC and CLC. (A) T2-weighted imaging shows homogeneous, moderately hyperintense lesion (arrows) with small necrotic focus. (B) In the arterial phase, the lesion shows moderate peripheral enhancement followed by (C) progressive contrast filling in the venous phase. (D) Muc-ICC showing abundant dense fibrous stroma. (E) T2-weighted imaging shows mixed intensity (peripheral, moderately hyperintense [arrows] and central hypointense [asterisk]). (F) In the arterial phase, the lesion shows heterogeneous, strong arterial enhancement followed by (G) progressive washout in the periphery of the tumor (arrows) and delayed enhancement in the center of the tumor (asterisk). (H) CLC showing hepatocytic differentiation area located in the tumor periphery (arrows) and ductular area located in the tumor center (asterisk).

further advantage was highlighted when we were able to classify the ICCs, even in large ICCs (mixed-ICC, 67.3 mm; CLC, 64.6 mm; muc-ICC, 41.2 mm); estimating the origin of the tumor using the current anatomical tumor classification becomes more problematic with increasing tumor size. These findings favor the proposed histological classification as a more accurate representative, reliable, and simple approach compared with anatomical classification.

Clinicopathological features differed in hilar CCs and muc-ICCs, compared with mixed-ICCs and CLCs. Mixed-ICCs and CLCs showed mostly a peripheral location, larger tumor size, less lymphatic invasion, and less perineural invasion. In contrast, hilar CCs and muc-CCs showed mostly a hilar location, smaller tumor size, more lymphatic invasion, and more perineural invasion. Immunohistochemically, the expression of S100P and cytoplasmic MUC1, reportedly prognostic markers for poor outcome in CCs[25,26] and other cancers,[27,28] was seen only in hilar CCs and muc-ICCs. In addition, TACSTD2 overexpression, reportedly an independent prognostic marker of poor outcome in several human carcinomas,[14,29] was more frequently seen in hilar CCs and muc-ICCs. This would suggest that hilar CCs and muc-ICCs are more aggressive when compared with mixed-ICCs and CLCs. This was supported by our *in vitro* data where the cell line corresponding to muc-ICCs had a significantly higher invasiveness compared with those corresponding to mixed-ICCs. The data indicate a clinical requirement to identify muc-ICCs from the other subtypes of CCs. Nonetheless, our data did not reveal a significantly different prognosis between the four groups, although the hilar CCs and muc-ICCs group tended to show worse prognosis compared with the mixed-ICCs and CLCs group. This may be due to the difference in the time of diagnosis in hilar CCs and muc-ICCs relative to mixed-CCs and CLCs. Because hilar CCs and muc-ICCs are mainly located in the liver hilum (associated with biliary problems), they can

be detected earlier when the tumor is smaller. This is also supported by the fact that the mixed-ICCs and CLCs tended to show larger tumor size and several nodules compared with hilar CCs and muc-ICCs. However, further investigation on the prognostic impact of mixed-CCs and CLCs in a larger study group is required.

In our series, one hilar CC and one mixed-ICC were diagnosed in the explanted liver. Hilar CC was found in a patient with PSC and with hilar BD stenosis, and the tumor was a periductal infiltrating type with moderately differentiated adenocarcinoma. A mixed-ICC of the mass-forming type and containing both hep-dif and ductular areas in the tumor was detected in a patient with hepatitis B– and C–related liver cirrhosis. Preoperative imaging of this ICC showed partial mimicking of a HCC-like pattern, such as early enhancement in the arterial phase and washout in the portal phase, and it was diagnosed as HCC and proceeded into liver transplantation without histological examination. Because ICC often shows lymph node metastasis (compared with HCC), it is not an indication for liver transplantation. However, in our series, all mixed-ICCs and CLCs showed mass-forming growth patterns and contained hep-dif areas in the tumor; these features may mimic HCC features in preoperative imaging. Mimicking of the HCC pattern has been reported with imaging in CLCs[30] and CCs.[31] In addition, our MRI data showed overlapping imaging characteristics between mixed-ICCs and CLCs. Therefore, histological assessment could be considered in patients who are hepatitis virus–positive and have a tumor with an atypical HCC pattern in preoperative examination.

To identify mixed features by preoperative needle biopsy, we studied five preoperative needle biopsies with a postoperative diagnosis of muc-ICC (n = 1) and mixed-ICC (n = 4). Three of the four mixed-ICCs were correctly diagnosed because they contained hep-dif or ductular areas together with a mucin-producing adenocarcinoma area. However, one biopsy was diagnosed as muc-ICC because the tumor sample contained only a mucin-producing adenocarcinoma area. We therefore conclude that if mixed features are detected in the biopsy, a mixed-ICC diagnosis can be made; however, the opposite is not always true.

In conclusion, about 39% of the ICCs studied presented with mixed features (hep-dif and ductular areas [mixed-ICCs]), whereas the remaining ICCs showed pure mucin-producing CCs (muc-ICCs). Mixed-ICCs showed similar clinicopathological, immunohistochemical, and gene expression profiles to CLCs (thought to be of HPC origin), and the immunohistochemical and gene expression profiles were similar to the most peripheral bile ductules. In contrast, muc-ICCs showed a similar profile to hilar CCs (so-called Klatskin tumor), and those profiles were similar to the mucin-producing cholangiocytes that line the hilar BD and intrahepatic large BD. These features probably reflect the different cell of origin. Histological classification may help in resolving the issues of current anatomical-based and pathological classification of CC. The immunoreactivity of S100P and NCAM represents a useful tool to distinguish mixed-ICC from muc-ICC.

References

1. Desmet V, Roskams T, Vos RD. Normal anatomy. In: Feldman M, ed. Gastroenterology and Hepatology. The Comprehensive Visual Reference. Philadelphia, PA: Current Medicine, Inc.; 1997:1.14.
2. Roskams TA, Theise ND, Balabaud C, Bhagat G, Bhathal PS, Bioulac-Sage P, et al. Nomenclature of the finer branches of the biliary tree: canals, ductules, and ductular reactions in human livers. HEPATOLOGY 2004;39:1739-1745.
3. Roskams T, Katoonizadeh A, Komuta M. Hepatic progenitor cells: an update. Clin Liver Dis 2010;14:705-718.
4. Komuta M, Spee B, Vander Borght S, De Vos R, Verslype C, Aerts R, et al. Clinicopathological study on cholangiolocellular carcinoma suggesting hepatic progenitor cell origin. HEPATOLOGY 2008;47: 1544-1556.
5. Nakanuma Y, Curado M-P, Franceschi S, Gores G, Paradis V, Sripa B, et al. Intrahepatic cholangiocarcinoma. Lyon, France: IARC; 2010.
6. Edge SB, Byrd DR, Compton CC, Fritz AG, Greene FL, Trotti III A. Perihilar Bile Ducts. 7th ed. Chicago, IL: Springer; 2010.
7. Han JK, Choi BI, Kim AY, An SK, Lee JW, Kim TK, et al. Cholangiocarcinoma: pictorial essay of CT and cholangiographic findings. Radiographics 2002;22:173-187.
8. Liver Cancer Study Group of Japan. Classification of Primary Liver Cancer. 1st English ed. Tokyo, Japan: Kanehara; 1997.
9. Levy M, Lin F, Xu H, Dhall D, Spaulding BO, Wang HL. S100P, von Hippel-Lindau gene product, and IMP3 serve as a useful immunohistochemical panel in the diagnosis of adenocarcinoma on endoscopic bile duct biopsy. Hum Pathol 2010;41:1210-1219.
10. Roskams T, De Vos R, Van Eyken P, Myazaki H, Van Damme B, Desmet V. Hepatic OV-6 expression in human liver disease and rat experiments: evidence for hepatic progenitor cells in man. J Hepatol 1998;29:455-463.
11. Okabe M, Tsukahara Y, Tanaka M, Suzuki K, Saito S, Kamiya Y, et al. Potential hepatic stem cells reside in EpCAM+ cells of normal and injured mouse liver. Development 2009;136:1951-1960.
12. Schmelzer E, Zhang L, Bruce A, Wauthier E, Ludlow J, Yao HL, et al. Human hepatic stem cells from fetal and postnatal donors. J Exp Med 2007;204:1973-1987.
13. Jozefczuk J, Stachelscheid H, Chavez L, Herwig R, Lehrach H, Zeilinger K, et al. Molecular characterization of cultured adult human liver progenitor cells. Tissue Eng Part C Methods 2010;16:821-834.
14. Fong D, Moser P, Krammel C, Gostner JM, Margreiter R, Mitterer M, et al. High expression of TROP2 correlates with poor prognosis in pancreatic cancer. Br J Cancer 2008;99:1290-1295.
15. Iemura A, Maruiwa M, Yano H, Kojiro M. A new human cholangiocellular carcinoma cell line (KMC-1). J Hepatol 1992;15:288-298.
16. Murakami T, Yano H, Maruiwa M, Sugihara S, Kojiro M. Establishment and characterization of a human combined hepatocholangiocarcinoma cell line and its heterologous transplantation in nude mice. HEPATOLOGY 1987;7:551-556.